Modelling the Maturation of Fentanyl Pharmacokinetics in Children

Sam Elder

A thesis submitted in partial fulfilment of the requirements for the degree of Master of Science in Pharmacology, the University of Auckland, 2024

Abstract

Aims: Fentanyl is a potent opioid analgesic used within the hospital setting for the management of acute pain within children following surgical procedures. The dosing of fentanyl in the paediatric population should be approached differently from new-borns up to children. The best approach for dosing fentanyl in this population remains unclear and required investigation. The aim of this thesis was to model the maturation of fentanyl pharmacokinetics, through simulated paediatric and adult data to assess the influence of age and size related changes. The aim was also model the changes in absorption fentanyl pharmacokinetics for nasal and Fentanyl Oralet formulations.

Method: Concentration-time data from 322 patients aged premature neonate to adult was simulated based on previous studies done within literature, to create a population dataset used for the analysis of fentanyl PK. Simulated concentration-time date was modelled to assess the influence of size and age covariates on predicting the clearance and volume of distribution for fentanyl. This data was modelled by 1, 2 and 3 compartment models for comparison to select the model of best fit. Size and age-related changes in clearance and volume were investigated using theory-based allometry with sigmoidal and linear maturation functions for clearance and volume. Concentration-time data from 122 adult patients receiving nasal administration of fentanyl and 33 child patients receiving fentanyl Oralet was used to describe fentanyl absorption pharmacokinetics.

Results: A 3-compartment model with a maturation function for clearance and volumes was selected as the most appropriate model for describing fentanyl pharmacokinetics from neonates to adults. Size and age covariates were shown to predict majority of the pharmacokinetic variability within fentanyl clearance and volume of distribution. Clearance was shown to increase with age and matured during the first year of infancy, reaching adult values after around 1 year post birth. Volume was shown to decrease with age, becoming elevated at birth and slowly decreasing towards adults' values after 1 year post birth. Absorption pharmacokinetics for both nasal and Fentanyl Oralet formulations were described however with some variability when compared to literature.

Conclusion: Size and age covariates can be used to reliably predict the pharmacokinetics of fentanyl from neonates up to adults. Use of a 3-compartment model best described the concentration-time data of fentanyl within this population. Further work is needed involving a pharmacodynamics-based model to describe the concentration-effect relationship of fentanyl, resulting in a link between dose and effect.

Acknowledgements

The process of completing my thesis this year has been challenging and demanding, and most certainly would not have been possible without the support I received from those around me.

To my supervisor Professor Brian Anderson, your knowledge, patience, and dedication kept me from spiralling throughout this year. It would be an understatement to say I was not the quickest student to learn however I wanted to say it has been a pleasure working with you this year, and my thesis would not be what it had become if it was not for your assistance and support throughout this year. Thank you, I appreciate it immensely.

To my fellow students in the pharmacometrics group in, thank you for your helpfulness in times of struggle and to see how I was getting on.

To my family, thank you for the unwavering support and confidence you give me, I could not do what I do without backing me.

Table of Contents

List of Figures

List of Tables

List of Equations

List of Appendices

1 Introduction

1.1 General outline and Aims

Paediatric patients (e.g neonates, infants, and children) experience acute pain following surgical procedures. Although the high incidence, the management of acute pain in this population is suboptimal, which can result in a higher frequency of adverse patient outcomes within the clinical setting [1]. Opioid analgesics such as fentanyl are most commonly used to treat moderate to severe acute pain within adult and children over 2 years of age, however the use of it within neonates and infants is mostly "off-label" globally and within the New Zealand healthcare system [2]. Unfortunately, the extrapolation of fentanyl data from adults into neonates, infants and children is not perfect, due to the biological differences present within the paediatric population compared to adults. Population models exist and an optimal dosing regimen of fentanyl in individuals, based on paediatric population data is needed. Abundant evidence exists for fentanyl use within neonates, infants, and children of various ages, using available population models e.g. discrete age bands, naïve pooled approach or two stage methods to describe the best dosing strategy. These currently available methods provide an overall understanding of fentanyl within the paediatric population. The aim of this study is to individualise the dosing of fentanyl within neonates, infants, and children, by determining the population PKPD and adverse effects.

The pharmacological effect of a drug is determined by the concentration reached within the plasma, and its effect at that concentration, therefore administering a dose which can achieve the desired fentanyl concentration, requires information regarding the balance between concentrations that produce analgesic and adverse effects. Pharmacokinetics (PK) is a discipline which is used to describe the relationship between drug dose and concentration within the body. The PK of a drug undergoes changes, with most drastic changes occurring in neonates and infants due to the maturation of physiological and biological systems throughout the body. Describing how the PK of fentanyl changes throughout development, and information regarding its non-IV formulations will be proposed to aid in informing a rational dosing regimen for improved fentanyl use in the paediatric population.

The aims of this study were to

1. Simulate a large population of patient concentration-time profiles consisting of neonatal to adult subjects from within existing fentanyl PK analysis studies

2. Describing changes in fentanyl CL and V with age and size, through the development of a pharmacokinetic population model using compartmental analysis

3. Describe the absorption characteristics of nasal and oral transmucosal fentanyl administration by estimating absorption half-life, lag time and bioavailability, through a pharmacokinetic population model

1.2 Fentanyl in children

The paediatric population (including neonates, infants, and children), all are subject to experiencing pain acute or chronic pain. Neonates specifically are frequently experiencing prolonged or repetitive pain within neonate intensive care units (NICU). Evidence is now even suggesting that neonates are more sensitive to pain than adults, and that insufficient management of pain in this population can be associated with short term complications and long term developmental problems in cognitive and motor areas [3]. Opiates have long been the standard for analgesia in the treatment of severe pain in children [4, 5]. Fentanyl and morphine are both opioid analgesics commonly used for the treatment of pain, however fentanyl has some advantages such as faster onset, less irritation and minimal effect on haemodynamic. Morphine is still the dominant opioid used for analgesia in children, as its elimination half-life is increased, resulting in a longer lasting effect then what would appear in adults [6]. Fentanyl's effect is short acting due to its rapid redistribution into tissue, and is eliminated slower within children due to immaturity of metabolic processes involved in its elimination [7]. This is why fentanyl is preferred by some for children and especially neonates experiencing acute pain , such as surgeries which requires mechanical ventilation[8]. Despite the common use of fentanyl in children, it has not been formally approved for use in this population. The Med Safe New Zealand data sheet for fentanyl citrate explicitly states that "fentanyl injection is indicated in adults and children aged above 2 years",

furthermore stating that “the safety of fentanyl in children younger than two years of age has not been established” [9]. Intravenous fentanyl is the most typical formulation used intraoperatively during general anaesthesia in adults however when treating children with fentanyl, different approaches are used. It has been well established that children associate injections and venepuncture as high anxiety and pain inducing events within the hospital [10]. As an alternative to avoid discomfort in the child, fentanyl is often administered intranasally, due to its ease of administration and its favourable PK for a non-intravenous method [11, 12].

1.3 Pharmacokinetics

The pharmacokinetic parameters clearance (CL) and volume of distribution (V) are useful for describing and calculating the dose that will achieve a concentration and desired effect of a drug. Linking the concentration of a drug to its desired effect is commonly referred to as the target concentration (TC) [13]. The volume of distribution and clearance are used to determine the loading dose and maintenance dose rates of a drug respectively. The use of pharmacokinetic parameters CL and V along with absorption parameters such as absorption half-life (Tabs) and bioavailability (F) are necessary to understand the time course concentration of a drug when compartment models are used [14]. These PK and absorption parameters can be influenced by patient-specific variables commonly referred to as covariates. Age and size are the most common covariates which are known to influence the CL and V of a drug. Additionally, formulation and administration route are factors which can also influence absorption parameters. Fentanyl PK has been investigated using both compartmental and non-compartmental population modelling methods, with non-compartmental methods seemingly being the preferred method within literature [15-19]. Compartment models which are used to investigate fentanyl pharmacokinetics can be comprised of a 1, 2 or 3 compartmental model [20-22] . The use of population modelling in conjunction with compartmental models allows for the pharmacokinetics analysis of a drug to better account for its disposition in the body and allows the use of effect and depot compartments which are useful for describing any delay between the drug concentration in plasma and effect.

Pharmacokinetic parameters are useful in simplifying the time-concentration profile of a drug into specific measures which are quantifiable. Traditionally, the use of non-compartmental analysis has been the standard method used for the estimation of PK parameters in population modelling for both children and adults [19]. Non-compartmental analysis has been favoured in the past as it requires less assumptions about the model and physiological system, while also being readily automated [23]. Modellers have begun to favour the use of compartmental models along with their associated parameters for the interpretation of fentanyl PK. Compartmental analysis estimates PK parameters using mathematical kinetic models and differential equations. As mentioned previously, compartmental analysis uses the PK parameters (CL, V, Tabs and F) to describe a one compartmental model, and non compartmental models. Furthermore, extra parameters are needed when describing additional compartments in a model, for example when using a two-compartment model, the parameters will consist of two volume parameters (V1, V2), a clearance parameter, and an intercompartmental clearance (Q). The parameters V1 and V2 simply describe the volume of distribution in each of the compartments, while Q describes the rate of drug transfer between the two compartments. Depictions of a one and two compartment model can be seen below (See Figure 1.1 and Figure 1.2).

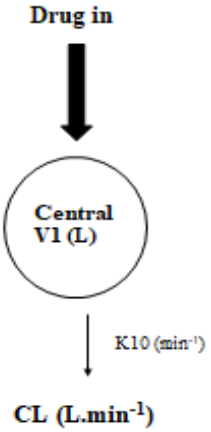

Figure 1.1: Schematic diagram for a one-compartment model

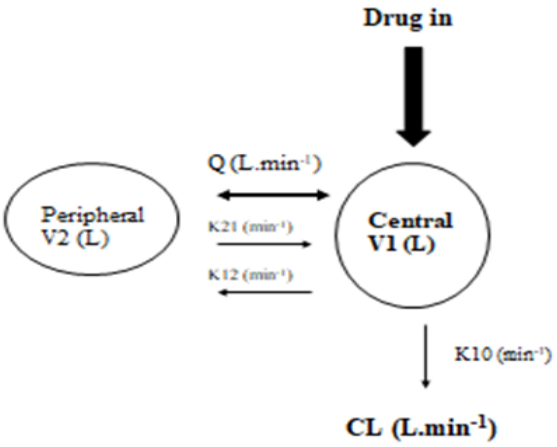

Figure 1.2: Schematic diagram for a two compartmental model

Non-compartmental modelling uses more confounded parameters which describe the exposure of a drug. For the non-compartmental modelling of fentanyl, the parameters commonly used are, maximum plasma concentration (Cmax), time to maximum plasma concentration (Tmax) and area under the concentration time curve (AUC), The parameters Cmax and Tmax are often used as they can be directly calculated from the observed data, and do not require equations for their estimation [18, 24].

1.4 Population modelling

Population modelling in pharmacokinetics plays a key role in estimating individual parameters from a single dose, which is useful for predicting the time-concentration profiles of other doses. When attempting to predict further out what will happen within a subject, the expected parameter values tend to differ, due to a factor accounting for interindividual variability between subjects is missing. If this variability between patients is modelled, then the magnitude of the difference can be predicted

between the predictions and observations in the next subject. There are three common approaches to modelling data collected from a group of subjects [25, 26].

1.4.1 Naïve pooled approach

The naïve pooled approach combines all time concentration data together as if all observations and doses belong to a single subject [27]. Sparse data from individuals are pooled into one data set and analysed as if the data were from one patient, which is then used for calculation of parameter estimates. This approach is typically used in scenarios where only one sample per patient is available. No individual information on subject profiles or parameters is obtained. This approach ignores any variability in the measured concentration therefore is only useful if there is extensive data for each of the individual concentrations and minimal between subject variability [27]. Problems occur with this method when data is missing from some of the subjects, which is common in measurements taken over longer periods of time or in subjects where sampling is less consistent i.e. neonates. Furthermore no information can be gathered about the size of between subject variability and its causes, this is due to inter-individual variability becoming indistinguishable from the residual error [28]. The basis for the naïve pooled approach is often not met when used, therefore the use of this modelling approach would generate incorrect parameter estimates.

1.4.2 Standard two-stage approach

The standard two stage method approach models concentration time data through analysis of individual profiles and structural parameters such as CL and V, for each measured concentration time profile and are then combine to achieve summary measure, such as the mean [27]. This approach requires a rich sampling dataset from each of the subjects within the analysis. Weighting summary measures can be performed however if the if the response for an individual is highly variable when compared to others if parameter estimates are derived from a different number of measurements in an individual. The between subject variability can be estimated from the standard deviation of the individual estimates, however this is an overestimate of the true variability because each estimate also has variability due to imprecision of the estimate (residual standard error). Covariates can be used to

explain some of the variability of the parameters however depends on having relatively good individual estimates of the parameters[27].

1.4.3 "True" Population modelling

Population modelling using mixed effects models [27, 29] has improved analysis and interpretation of PKPD data. Mixed effect modelling is used to describe the variability present in concentration-time data, with addition of fixed and random effects. Fixed effects such as explanatory covariates (e.g. age, size, renal function, sex, fat mass) can be introduced that explain the predictable part of the between-individual variability for each of the parameters [27]. Random effects are included to describe inter-individual variability and random residual variability , which is unable to be predicted through fixed effects [30]. This approach treats the population, rather than as individuals. Sparse data samples (1-3) are used over rich data samples (6+) as they can be obtained and analysed from a larger cohort of individuals, resulting in a more representative sample of the target population [27]. This approach also allows for the ability to improve the predictions for individuals from "special" populations such as paediatrics. Studies and pharmacokinetic data from paediatric populations is often much less available when compared to adult studies, even when the data is available, the study populations tend to be much smaller [27]. Sampling times are not crucial for this method and sampling time windows rather than exact times are as equally effective for this approach, which allows flexibility in child population groups [31]. Population modelling also allows pooling of data across different studies to provide a single robust PK analysis rather than comparing separate smaller studies that are complicated by different methods and analyses. Mixed effect modelling is typically performed using nonlinear mixed effects modelling statistical software (NONMEM). Nonlinear regression is performed by an iterative process to find the curve of best fit [32, 33].

1.5 Covariates

Population PK/PD modelling allows for the analysis of the relationship between independent demographic variables (covariates) and pharmacological parameters (CL and V). Covariates are used to explain the predictable portion of inter-individual variability within a population. Covariate

analysis can become challenging when one covariate can trump the effect of other covariates of interest, or patient specific data is missing that is important in characterising the population. It is also possible that some covariates are closely related, making it difficult to estimate parameters, this is typically denoted as collinearity. Size and age (maturation) are two common covariates used to explain pharmacokinetic variability when comparing paediatrics to the adult population.

1.5.1 Size

Changes in size within children reflect weight and height factors which can be easily measured and quantified. Weight is the main factor when it comes to predicting clearance and volume of distribution in an individual, which are two parameters that heavily influence the concentration time profile of a drug. Due to this influence on the concentration time profile, the dose given to a patient is usually adjusted to their weight (kg). Clearance is a parameter representative of the metabolic processes in the body and has been observed to change very rapidly in children. Clearance in children 1-2 years of age, commonly expressed as L/min/kg, is commonly greater than that observed in older children and adolescents [34]. This is due to a size effect and is not accredited to larger livers or increased hepatic blood flow in within the paediatric population. Historically, this difference in clearance within the paediatric population has been ignored. The linear per kilogram and body surface area (BSA) size models have been traditionally used for the scaling of clearance, however these models assume clearance is directly proportional to bodyweight, which has been refuted heavily within current literature [30, 34-36]. To compensate for these size effect changes seen in this subpopulation, allometric scaling is used. Allometric scaling states that a pharmacokinetic parameter can be related to the individuals body weight by the PWR exponent. Allometry is a term used to describe the nonlinear relationship between size and function. The value of PWR describes how the parameter of interest (clearance) scales over different values of body size. The PWR value is most associated with the parameter of metabolic processes. This value of PWR has been the subject of much debate, with either a *PWR* value of 2/3 (i.e. body surface area) or a value of ¾ considered to be better for the scaling of body size. For allometric scaling, the ¾ method is used for metabolic processes, 1 for physiological volumes, and ¼ for time related indices [37]. Support for a value of ¾ comes from

investigations that show the log of basal metabolic rate (BMR) plotted against the log of body weight produces a straight line with a slope of ¾ in all species studied, including humans [34]. Structural and time related variables scale predictably within and between species with weight (*W*) exponents (*PWR*) of ¾ , 1 and 1/4 respectively [37]. These different exponents used as the PWR values can be applied to different pharmacokinetic parameters such as (CL exponent of 3/4) and volume (V exponent of 1) [37]. Allometric scaling for body size is advantageous over other methods in multiple aspects. Firstly, allometric models provides more accurate scaling of pharmacokinetic parameters over a vast range of body weights, which is important for dose extrapolation within children whom pharmacokinetic parameters are different to adults. Secondly allometry uses fixed PWR value exponents which allows for secondary covariate effects such as age to be defined independently of size [29]. Additionally, allometry allows for direct comparisons of adult and paediatric pharmacokinetic parameters when a weight standard 70kg is used. The exponents 3/4, 1 and 1/4 can also all be applied to various PK parameters for determination of the factor of size.

1.5.2 Age

The method of allometry alone, is insufficient in its ability to predict clearance within the paediatric population, especially for neonates and infants. The addition of age in relation to maturation and weight is known to influence the clearance of drugs within this population, which is why age is an important covariate to consider [38]. The relationship between maturation and clearance proves more difficult to predict when compared to the relationship between size and clearance. Age is commonly defined in relation to development of an individual, which in neonates and infants is a rapidly dynamic process. Development occurs both during intrauterine and extrauterine life for a neonate. Defining when the conception of a foetus is inconsistent which is why post-menstrual age (PMA) is used. PMA is defined by the last menstrual period post conception and is more commonly used for determining biological age than post-natal or gestational age [7, 34]. Understanding maturation of organs such as the kidneys and liver is important, as these organs are critically involved in drug clearance processes. The glomerular filtration rate (GFR) is a measure of how well the kidneys are functioning. In premature and mature neonates, the GFR matures relatively slowly, reaching ~25% of adult

function around the time birth occurs (40 weeks PMA) [39]. CYP metabolising enzymes are also affected by maturation, with many of them varying in their activation times. CYP3A4 is important in the metabolism of a large majority of endogenous compounds and drugs such as fentanyl [40]. CYP3A4 is functionally immature at birth in neonates and only begins to increase its expression after ~2 weeks PNA and reaches around 30-40% of adult expression by ~4 weeks PNA.[40] Subsequent changes in CYP3A4 expression are not then seen until after the first year of life, and reaches adults levels of expression by ~2 years of age [41]. Most other maturation changes are complete within the first 2 years of PNA.[34] Both GFR and CYP maturation are heavily influential on the clearance of an individual, which is an important factor for determining the appropriate dose of a drug.

The influence of age on volume is also important to include when discussing covariates to consider for neonates and infants. Fentanyl is highly lipophilic drug, which is why rapid redistribution into fat and muscle occurs. Neonates and especially preterm neonates have a lower percentage of fat and muscle in proportion to weight, when compared to adults [42]. The percentage of body weight which contributes to fat in a 1.5 kg preterm neonate is ~3% and 12% in a term neonate, compared to an 70kg adult where ~20% of body weight is contributed to fat [42]. These low percentages of fat in preterm and term neonates compared to adults' results in a higher volume of distribution for lipophilic drugs such as fentanyl. Volume changes begin to occur after birth which is why post-natal age (PNA) is used over PMA for describing the maturation profile of volume from preterm neonate to adult.

1.6 What is known about PK in children

The impact of size on fentanyl pharmacokinetic parameters clearance and volume of distribution has been investigated previously but did not provide a coherent quantification [35]. Ziesenitz et al (2018) showed that size is a primary indicator for predicting fentanyl clearance and volume of distribution and explaining its variability from pre term neonates to infants [35]. The clearance and volume of distribution at these ages were shown to have reached full maturity (adult values) when standardised to a 70kg individual using an allometric scaling method. Age is also known to be a factor which influences the

clearance and volume of distribution of fentanyl, particularly in neonates and infants within the first two years of life (see 1). This makes extrapolation of clearance and volume parameters, using strictly size alone for neonates and infants unreliable and unjustified. Wu et al (2022), characterised importance of pre and postnatal maturation on the pharmacokinetics of fentanyl across preterm and term neonates aged (24 weeks to 42 weeks PMA)[43]. Size and age were found to be an important predictor for both clearance and volume of distribution in this population [43]. Allometric scaling in this study involved birthweight (BW) and post-natal age (PNA) as power exponent relating to how clearance and volume changes with birthweight (BW) and post-natal age (PNA) [43]. A lack of child and adult subject data in this pooled population approach study makes extrapolation of clearance and volume parameters across an entire population impossible and therefore unconventional for an individual dose-based approach.

2 Simulation of Time-Concentration Profiles

2.1 Aim

As discussed, prior, fentanyl is an opioid analgesic used off-label in neonates, infants, and children to treat severe acute pain in a hospitalised setting. Published estimates of pharmacokinetics parameters clearance and volume of distribution in adults and children of different ages were available and were reviewed in this chapter. To create an effective population PK model for fentanyl, a large pool of patient data will be required to represent a population. This patient data will be all be taken from available previous studies involving fentanyl PK in children and adults. This patient data will include age, weight, dose, and crucially concentration time data. The concentration time data for each patient is important as it is necessary to estimate PK parameters (CL and V), which will be used to inform the dosing of fentanyl in the paediatric population. Unfortunately, it is uncommon to find studies which provide the raw data for each of the patients, this includes concentration-time data. To circumvent this, the concentration-time profiles for each of the patients can be simulated through the modelling software NONMEM. For each study, the simulation of concentration-time data will utilise the PK parameter estimates of the population for that study.

The aim of the work described in this chapter was to:

1. Search online databases for studies involving compartmental fentanyl pharmacokinetic, with published PK estimates (CL and V).

2. Create NM-TRAN simulation control files for each of the studies using the published PK estimates

3. Simulate individual patient fentanyl concentration-time data using NONMEM

2.2 Literature search

Pharmacokinetic studies involving fentanyl use conducted in children were identified from a literature search in PubMed, using the following search terms and key words to identify the most appropriate studies: Fentanyl, Pharmacokinetics, PK, Population modelling, Children, Neonate(s), Paediatric(s), Infant(s), Review, Postnatal, Postmenstrual, Gestational, Preterm, Population, Analysis, Modelling.

Data collated from the literature was formatted in such a way that was suitable for analysis through the NONMEM software.

a). Identification of PK parameter values CL and V from the literature review, for children between the ages of 0-18 years. An attempt to use papers which defined CL and V values for individuals was done. However, not all papers provide this data and other studies simply define mean values or instead, non-compartmental parameters values such as AUC or T1/2. Papers which supplied these non-compartmental parameters will require conversion to CL and V. An excel spreadsheet from this was created and included parameters estimates (CL and V), weight (kg), age and, formulation.

b) Literature parameter values reported for clearance and volume were used to simulate individuals and create time-concentration profiles in subjects (premature neonates to adolescents).

c) Time-concentration profiles for individuals or naïve pooled analysis groups, when available in literature, was also added to the simulated data

d) PK analysis of fentanyl included data (e.g. Wu et al) that included maturation models where the exponent on weight changes with age, rather than the more conventional maturation model (See Chapter 3). Simulation of these data using this non-conventional model was possible and included the neonatal cohort.

Table 2.1: Published literature estimates of fentanyl clearance within individuals aged premature neonate to adult. Estimates have been standardised to a 70kg individual

Study	**Patients (n)**	**PMA (weeks)**	**Weight (kg)**	**CL presented (units)**	**CL std (L/min/70kg)**	**Q2, Q3 (L/h/kg)**
***Wu et al*[43-45]**	164	24.14 - 41.86	0.49 - 4.05	0.315 L/h	0.00525	0.00596
***Koehntop et al*[46]**	1	40.14	3.2	26.8 ml/kg/min	0.0858	-
	1	40.14	3.3	20.1 ml/kg/min	0.066	-
	1	40.14	3.5	5.4 ml/kg/min	0.019	-
	1	40.14	4	58.7 ml/kg/min	0.235	-
	1	40.29	3.3	9.8 ml/kg/min	0.032	-
	1	40.29	3	13.4 ml/kg/min	0.04	-
	1	40.29	2.6	3.4 ml/kg/min	0.0088	-
	1	40.29	2	9.1 ml/kg/min	0.018	-
	1	40.29	3.5	10.7 ml/kg/min	0.037	-
	1	40.29	1.9	8.02 ml/kg/min	0.015	-
	1	41	3.8	12.8 ml/kg/min	0.049	-
	1	41	3	20.0 ml/kg/min	0.05	-
	1	41	3.4	5.5 ml/kg/min	0.012	-
	1	41	3.7	47.4 ml/kg/min	0.066	-
***Johnson et al*[47]**	2	40.14	3.1-3.17	16.2 ml/kg/min	0.051	-
	2	57.42-58.9	6.07-6.1	18.1 ml/kg/min	0.107	-
	6	170-210	14.5-17.5	11.5 ml/kg/min	0.198	-
	3	664-679	57.4-58.8	7.05 ml/kg/min	0.411	-
	4	1199-1355	73.7-80.2	10.0 ml/kg/min	0.799	-
***Foster et al*[48]**	24	2588-3680	58-130	2.31 L/min	1.4	
	24	-	-	1.41 L/min	0.667	0.918
	24	-	-	1.28 L/min	1.28	3.35
***Loughren et al*[49]**	16	2588-3680	64-98	0.96 L/min	0.522	0.957, 0.799
***Scott et al*[50]**	20	1080-4616	64-130	637 ml/min	0.207	0.268
***Lim et al*[51]**	19	1444-3264	52-90	2.4 L/min	2.4	-

Table 2.2: Published literature estimates of fentanyl's volume of distributions within individuals aged premature neonate to adult. Estimates have been standardised to a 70kg individual.

Study	**Patients (n)**	**PMA (weeks)**	**Weight (kg)**	**V1 (units)**	**V2, V3 (units)**	**Vdss (units)**	**V1 std (L/70kg)**	**V2, V3 std (L/70 kg)**
***Wu et al*[43-45]**	164	24.14 - 41.86	0.49 - 4.05	10.6	3.37	-	14	3.37
***Koehntop et al*[46]**	1	40.14	3.2	-	-	2.69 L/kg	8.61	-
	1	40.14	3.3	-	-	3.42 L/kg	11.2	-
	1	40.14	3.5	-	-	2.66 L/kg	9.1	-
	1	40.14	4	-	-	9.85 L/kg	39.4	-
	1	40.29	3.3	-	-	1.34 L/kg	4.42	-
	1	40.29	3	-	-	3.8 L/kg	11.4	-
	1	40.29	2.6	-	-	1.69 L/kg	4.39	-
	1	40.29	2	-	-	4.88 L/kg	9.76	-
	1	40.29	3.5	-	-	7.1 L/kg	24.9	-
	1	40.29	1.9	-	-	10.49 L/kg	19.9	-
	1	41	3.8	-	-	2.2 L/kg	8.36	-
	1	41	3	-	-	5.52 L/kg	13.8	-
	1	41	3.4	-	-	2.3 L/kg	4.83	-
	1	41	3.7	-	-	13.46 L/kg	18.8	-
***Johnson et al*[47]**	2	40.14	3.1-3.17	-	-	5.94 L/kg	18.9	-
	2	57.42-58.9	6.07-6.1	-	-	4.45 L/kg	26.5	-
	6	170-210	14.5-17.5	-	-	3.06 L/kg	52.9	-
	3	664-679	57.4-58.8	-	-	1.92 L/kg	111	-
	4	1199-1355	73.7-80.2	-	-	1.61 L/kg	125	-
***Foster et al*[48]**	24	2588-3680	58-130	99 L/kg	-	-	99	-
	-	-	-	9.07L/kg	63L/kg	-	9.07	63
	-	-	-	80 L/kg	123 L/kg, 815 L/kg	-	80	123,815
***Loughren et al*[49]**	16	2588-3680	64-98	12.4 L	16.9 L, 186 L	-	32	19.8,147
***Scott et al*[50]**	20	1080-4616	64-130	12.7L	-	339 L	14.65	386

***Lim et al*[51]**	19	1444-3264	52-90	27.0 L/kg	-	32.6 L/kg	27	32.6

2.3 Simulation to build up data base

Simulation of the individual concentration data using non-linear mixed effect modelling (NONMEM 7.4, ICON Development Solutions, Hanover, MD, USA). Simulations were conducted using the Monte Carto method. The Monte Carlo simulation is a probabilistic model that can make predictions which include an element of randomness or uncertainty [52]. The method is beneficial for the simulation of clinical data, random data as it simulates large pools of random data from a statistical distribution (log-normal) based on the fixed estimates set (CL and V). Demographic information from the 7 studies used for this simulation (see Table 2.1), were pooled and resampled to create a simulation data file. The demographic information for each patient included; age, weight, post-menstrual age, post-natal age, and gestational age. The age range of subjects across the 7 studies was from 1-day old new-borns, up to 88 years of age. Simulating both neonatal and adult concentration data was important for the population modelling of fentanyl, which leads on from the simulation step. Fentanyl concentrations were simulated at time points like what was previously done in each study, as the aim was to emulate each studies concentration profiles. All fentanyl concentration measurements were taken after administration. Fentanyl concentrations were simulated at time points ranged between 0 and 3600 minutes. The administration of fentanyl in these studies included some using single bolus dosing and some using infusions over different time periods.

Pharmacokinetic information was published within each of the 7 studies used, which was used in the simulation of fentanyl concentration time data. The studies included in the simulation were a variety of 1, 2 and 3 compartmental analyses. The pharmacokinetic information from these studies included compartmental parameters CL and V, as well as additional parameters V2, Q1, V3 and Q2 for the 2 and 3 compartmental studies. Many of these studies presented their clearance and volume estimates as

parameters for the entire study population, however some of the studies did provide estimates for each individual within that study (See Table 2.1 and Table 2.2). Each of the studies presented their clearance and volume estimates in varying ways, resulting in different units of measurement across the 7 studies, requiring standardisation. For clearance, prior to simulation all presented estimates within the studies were converted to an allometric theory to a standardised litres per minute measurement for a 70kg individual (L/min/70kg) (See Table 2.1). For volume, all presented estimates were converted to a standardised litre measurement for a 70kg individual (L/70kg) (See Table 2.2).

The demographic and pharmacokinetic information published within each study was collected and used for the simulation of fentanyl concentration time data. The information provided within each study was the following.

2.3.1 Study 1; Wu et al

Pharmacokinetic data was available from 164 newborns, (age range 24.14 – 41.86 weeks post-menstrual range (PMA)) and (weight range 0.39 – 4.25 kg) which was pooled from two previous studies for a population pharmacokinetic study [43]. All 66 neonates within the first study received an initial 1-h infusion of 10.5ug/kg fentanyl, followed by a continuous infusion at a constant rate of 1.5ug/kg/h for median duration of 58h. Blood samples were taken at time 0 of the initial infusion, and 1, 2, 12 ,24 ,48, and 60 hours after the initial infusion of fentanyl. The second study included the remaining 98 subjects from this pooled analysis. Of the 98 preterm infants, 69 received a bolus dose only, 9 received a continuous infusion and the remaining 20 received both a bolus and infusion dose. For the bolus dose, a single bolus dose of 2 ug/kg was administered. For the infusion, a continuous infusion of 1 ug/kg/h was administered for a duration of 23h. Blood samples for the bolus only subjects were taken at time 0 of when the bolus dose was administered, and at 1, 2, 4, 10, 16 and 24 hours after bolus administration. Sampling for the infusion only and bolus + infusion subjects were taken at the start of the infusion at time 0, and at 1, 2, 12, 24, 48 and 60 hours after start of infusion.

2.3.2 Study 2; Koehntop et al

Pharmacokinetic data was available from 14 neonates undergoing major surgical procedures [46]. Patients were aged 40.14 – 41 weeks PMA and weighed 1.9 – 4 kg. Participants received an intravenous fentanyl injection of 10ug/kg (n=1), 25ug/kg (n = 4) or 50ug/kg (n=9). The 25ug/kg and 50ug/kg doses were administered via injection over a 3-minute period to ensure hemodynamic stability within the participants. Blood samples were taken at initial fentanyl administration at time 0, and at 1, 2, 5, 10, 20, 40, 60 minutes and 2, 3, 4, 8 and 12 hours after fentanyl administration.

2.3.3 Study 3; Johnson et al

Pharmacokinetic data was available from 17 subjects, which were studied within 5 different groups categorized by age [47]. (Group 1 n = 2 : 0 - 1 month, Group 2 n = 2 : 1 month – 1 year, Group 3 n = 6: 1 year – 5 years, Group 4 n = 3: 10 years – 14 years, Group 5 n = 4: 20 years – 35 years). Each of the groups also contained multiple patients with weight ranges (Group 1 = 3.1 – 3.17 kg, Group 2 = 6.07 – 6.1 kg, Group 3 = 14.5 – 17.5 kg, Group 4 = 57.4 – 58.8 kg, Group 5 = 73.7 – 80.2 kg). All participants received a 2–7-minute intravenous infusion of fentanyl, with the dose varying for each group (Group 1 = 30.3ug/kg, Group 2 = 19.1ug/kg, Group 3 = 10ug/kg, Group 4 = 4.34ug/kg and Group 5 = 15.9ug/kg). Blood samples were taken at initial fentanyl administration at time 0 and at 2, 5, 7, 10, 15, 30, 60 minutes and 2, 3, 4 and 8 hours after fentanyl administration.

2.3.4 Study 4; Foster et al

Pharmacokinetic data was available from 24 subjects (49 – 70 years) given fentanyl during oral surgery [48]. Participants received an intravenous 75, 100, 150 or 200ug bolus dose of fentanyl. Participants received the 75 or 100ug dose over 1 minutes, while the 150 and 200ug doses were administered over 6 minutes. Blood samples were taken at time 0 of fentanyl administration and at 5, 10, 15, 20, 30, 40, 60, 75, 90, 120, 150, 180, 240 minutes after fentanyl administration.

2.3.5 Study 5; Loughren et al

Pharmacokinetic data was available from 16 subjects (21 – 41 years) given fentanyl with and without the addition of St. John's Wort [49]. Participants received a fixed-dose 2.5ug/kg intravenous infusion of fentanyl for 30 minutes. Blood samples were taken at the start of infusion at time 0 and at 5, 10, 15, 20, 30, 40, 60, 75, 90, 120, 150, 180 minutes after the start of infusion.

2.3.6 Study 6; Scott et al

Pharmacokinetic data was available from 20 subjects (20 – 88 years) given fentanyl when undergoing elective surgery [50]. Participants received an intravenous infusion of 150ug/min fentanyl. Infusion was terminated when there was appearance of delta waves in raw EEG tracing. This resulted in the duration of infusion being 5 minutes for each of the subjects. Blood samples were taken at the start of infusion at time 0 and at 1, 2, 4, 5, 7, 9, 12, 14, 16, 18, 20, 25, 30 minutes after the infusion began.

2.3.7 Study 7; Lim et al

Pharmacokinetic data was available from 18 subjects (27 – 62 years) given fentanyl during and post operation [51]. Participants received an intravenous 50ug bolus dose of fentanyl over a 1-minute period. Blood samples were taken at fentanyl administration time 0 and at 2, 5, 10, 15, 20, 25, 30 minutes after the dose was given.

2.4 Process of simulation

To perform a simulation using NONMEN, two files must be created for each set of data desired to be simulated. The first file necessary for NONMEM simulation is a simulation dataset file. This is a Microsoft Excel.csv (comma-separated values) file which contains all dosing and demographic information for everyone simulated, this includes; amount (ug) , time of sampling, rate of infusion if applicable, and duration of dose (minutes). Key demographic information within the dataset file included; weight (kg), post-menstrual age (weeks), post-natal age (weeks) and gestational age (weeks). The second file necessary for NONMEN simulation is a NONMEM control file. The control file is comprised of NM-TRAN code which outlines the components of the appropriate structural model e.g.

2-compartment intravenous bolus PK. These components include; parameters, dosing and sampling, integration, and simulation. NONMEM provides a library of pre-written PK models, which can be utilised to solve pharmacokinetic problems. The library of models is called Predictions for Population Pharmacokinetics (PREDPP). The use of PREDPP requires 3 components within the control file; $SUBR, $PK and $ERROR. The first is $SUBR, which specifies which PREDPP subroutine to use and how it should be parameterised. The ADVAN subroutine outlines the model type (number of compartments) and the TRANS subroutine determines the parameters that need to be defined for the $PK. ADVAN subroutines are advantageous as they advance the solution of the model from one record in the data file, to the next in a time sequence. This was useful for simulation as the dosing patterns across all the studies were not uniform, meaning ADVAN was able to correct for this. The second component $PK, specifies the individual pharmacokinetic parameters. This involves a fixed effect model denoted as THETA (n) and a random effects model for the population parameter variability denoted as OMEGA (n). The names of the individual parameters used in $PK are defined within the selected PREDPP and must match what is indicated in $SUBR. The third component $ERROR, specifies a model for residual error random effect, to describe the variability between individual predictions and the observations. For all simulations a combined error model was used.

2.5 Results

The dosing and demographic information for everyone, in combination with the population PK parameter estimates, allowed fentanyl concentration time data to be replicated for each of the 7 studies, through simulation. A total of 322 patients were simulated across the 7 studies, resulting in a total of 3016 concentration measurements being generated through simulation. Of the 322 patients, 182 were paediatric patients ($\leq$2 years of age) and 140 were adult. The concentration-time data simulated was intended to agree with the concentration-time profiles published in the source material used for the simulation. The raw concentration-time profile data per individual was not provided by any of the source material, instead the studies provided time-concentration graphs as the sole method of displaying their results. It was important for the simulated concentration-time data to agree with the original data in the source material, as the whole purpose of the simulation step was to create a large database of

fentanyl concentration-time profiles for pharmacokinetic analysis. Validation of the simulated concentration-time profiles was done by visual comparison to the provided concentration-time graphs available in the source material.

Mean concentration was calculated using the available simulated fentanyl concentration samples. The studies used a variety of sampling times inconsistent with one another making it difficult to omit any specific time points of samples. All 3016 simulated fentanyl concentration samples were used in the determination of the mean. Full time-concentration profiles of randomly selected individuals from the simulation can be seen below in Figure 2.1. The control files used for the NONMEM simulations of each study are provided in the Appendix and are labelled as Appendix 1 – 7.

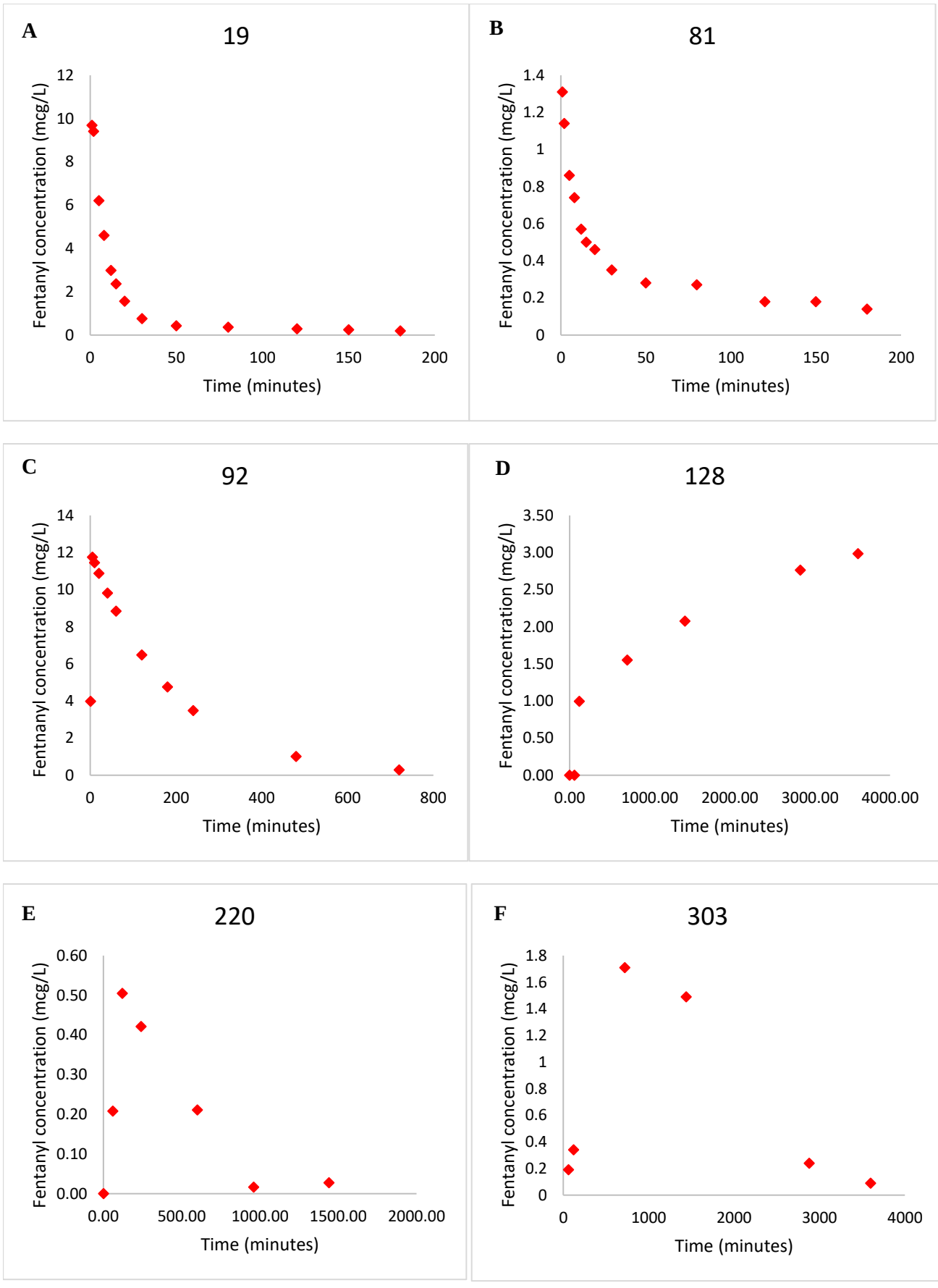
A
19
Fentanyl concentration (mcg/L)
Time (minutes)
B
81
Fentanyl concentration (mcg/L)
Time (minutes)
C
92
Fentnanyl concentration (mcg/L)
Time (minutes)
D
128
Fentanyl concentration (mcg/L)
Time (minutes)
E
220
Fentanyl concentration (mcg/L)
Time (minutes)
F
303
Fentanyl concentration (mcg/L)
Time (minutes)

Figure 2.1: Individual concentration time profiles of subjects 19, 81, 92, 128, 220 and 303, simulated by NONMEM. **A:** 67 year old patient received 100ug bolus dose, **B;** 49 year old received a 100ug dose **,C;** 4 day old new-born received a 150ug infusion over 3 minutes, **D;** 25 week PMA preterm neonate received a 10.5ug/kg infusion for an hour, followed by a 1.5ug/kg/h continuous infusion for the following 59 hours, **E;** 31 week PMA preterm neonate received 2ug/kg bolus dose, **F;** 30 week PMA preterm neonate received 2ug/kg bolus dose followed by a 1ug/kg/hr continuous infusion for 23 hours.

The raw concentration-time data was chosen at random from 6 individuals within the final simulation database. Of the 6 randomly chosen individuals, 2 adults and 4 paediatric patients were picked. The 6 individuals were all picked to be from different study simulations to show a wide sample of concentration data between all the studies. The concentrations for each individual were simulated through NONMEM and are based off the PK parameter estimates which were available in the published literature (see Table 2.1 and Table 2.2).

2.6 Discussion

Fentanyl concentrations for the population were successfully simulated using NONMEM. The simulated fentanyl concentrations were predicted using the parameters provided by each of the studies (see Table 2.1 and Table 2.2). The patient profile sets provided by these studies included a wide distribution of participants, ranging from 1-day old pre term neonates, up to 60+ year old adults. The simulation done in this chapter was to create a large population dataset of fentanyl concentration profiles consisting of individuals within all age ranges. The concentration-time profiles for the simulated patients (See Figure 2.1) were validated by comparison of these profiles to what was provided within each of the corresponding studies the data was simulated from. These concentration-time profiles are noticeably different from one another, due to difference in the dosing and sampling methods for each of the studies. Comparison of the concentration values across studies was not beneficial, due to different dose amounts, bolus and/or infusion methods, length of sampling and population differences between paediatric and adult subjects. Ultimately all the concentration data simulated was combined into a datafile which was to be used for the estimation of population pharmacokinetic parameters, and to assess how these change with age and size.

It was expected that the parameter estimates within the studies involving children, would be different to those from the adult population studies. The parameter of clearance is known to be smaller at birth, and typically matures to adult values after ~1 year post-natal [53]. The clearance estimates for each of the studies within Table 2.1 agree with this idea of increasing clearance maturation with age, when standardised to a 70 kg individual. The clearance estimates from the paediatric studies Wu et al and Koehntop et al presented lower than the clearance estimates presented by the adult studies such as Foster et al and Loughren et al [43, 46, 48, 49]. The determination of clearance within the Wu et al study was approached from a method different to a standard ¾ power allometry for a 70kg individual. For the covariate analysis conducted within the Wu et al study, the implementation of a combined BW (birthweight) and post-natal age function, best described the maturation of clearance within their preterm neonatal population. A function more commonly used for describing clearance maturation in newborns involves post-menstrual age. This function makes the assumption that maturation of a neonate begins in utero rather than at birth, therefore post-menstrual age describes the age of a neonate starting at the last menstrual cycle experienced by the mother [37, 38]. Based on the PNA and BW regimen used in this study, the range of concentration of fentanyl among all neonates reported in this study was (0.3 – 3.1 mcg/L) [43]. The results of the simulated fentanyl concentration data for this study using the same PNA and BW regimen were within this range, with a mean concentration (1.02 mcg/L) for all 166 subjects.

The parameter of volume presented within these studies was also expected to vary between paediatric and adult published data. The volume of lipid-soluble drugs such as fentanyl, within neonates is higher at birth and decreases with age, due to the increasing volume/kg of muscles and fat as the new-born matures [54]. The volume estimates for each of the studies within Table 2.2 were varied across the paediatric and adult studies when standardised to L/70kg. Johnson et al reported volume of distribution estimates which increased with age when allometry was considered, which contradicts the expected decrease mentioned before that should be seen for a highly lipophilic drug such as fentanyl. The authors attributed this contradiction to potential age related differences in tissue perfusion and/or tissue sequestration [47]. There may be inaccuracies in estimating the volume within children $\geq$ 2 years of age,

particularly newborns, however there is little evidence to suggest tissue perfusion attributing to volume estimates becoming lower than adult values. Utilization of a physiologically-based pharmacokinetic (PBPK) model could potentially aid in describing this anomaly of increasing volume with age [55]. Ginsberg et al evaluated volume differences between adult and paediatric data across a database of 22 chemicals [53]. They found the trend was that children have a greater volume than adults, and was fairly consistent across all chemicals, lipophilic and hydrophilic [53].

3 A Universal Pharmacokinetic Model of Intravenous Fentanyl

3.1 Introduction

Published estimates of pharmacokinetic parameters clearance and volume for fentanyl in infants and adults have been previously reviewed (See Tables Table 2.1 Table 2.2). Paediatric studies investigate the pharmacokinetics of fentanyl were available, however many of these studies employ non-compartmental analysis, which has been proven to poorly investigate PK variability. Results from non-compartmental analyses complicate interpretation of PK for between study comparisons due to large unexplained variability, which is not useful for a population modelling approach. There are studies available which have employed compartmental analysis to investigate the PK of fentanyl within the paediatric population. The common practice of body weight-based dosing in this population does result in varying concentrations over time across children, especially neonates and infants. The studies which are available are solely basing their dosing off bodyweight, and are not investigating the impact of size and age on their dosing approaches. Several studies have been conducted for the analysis of fentanyl in children. One analyses has been published previously for preterm neonates, a study conducted by Wu et al, a pooled population pharmacokinetic analysis of preterm neonates aged (24-42 weeks gestational age). These analyses used a formula based on birthweight and post-natal age as a descriptor for size on clearance, rather than allometric scaling [43]. Two other useful analyses involving children have been published previously. One conducted by Koehntop et al in neonates aged (1-7 days post-natal age), and another by Johnson et al in infants aged (1 day to 3 years) and included a group of 12 and 27 year old patients [46,47]. These studies either did not incorporate, or included very limited adult population data into their analyses. The maturation profile of fentanyl clearance and volume of distribution from birth to adulthood remains to be described within infants. Given this limited PK information across the entire paediatric population, the PK profile of fentanyl across the entire paediatric population will be characterized to individualise dosing.

A population compartmental model which describes the pharmacokinetics of intravenous fentanyl from birth to adulthood would be useful for:

a) describing changes in fentanyl CL and V with age and size, which are important in the calculation of drug dosing

b) validating and understanding currently available literature

The aim of the work described in this chapter was to:

1. develop a population model to describe the pharmacokinetics of fentanyl from birth (e.g., premature neonates) to adulthood and investigate the impact of covariates size and age, on pharmacokinetic variability

2. determine whether a 1,2 or 3 compartmental population model produces the best estimates for the population pharmacokinetics analysis

3. compare population pharmacokinetic parameter estimates with those that are available within literature for

3.2 Methods

Non-linear mixed effect models were constructed and used for the pharmacokinetic analysis of intravenous fentanyl. Model building for non-linear mixed effects involves the process of determining the characteristics for both the fixed and random effects of a population, while still managing to include individual differences within that population. Analysis of the individual PK data using non-linear mixed effect modelling (NONMEM 7.4, ICON Development Solutions, Hanover, MD, USA). NONMEM is used to define the population distribution of PK parameters (e.g. CL and V) through estimation of the population characteristics. Population pharmacokinetic parameters, covariate effects, between subject and residual variances were all estimated using the first order conditional method with interaction (FOCEI). Estimation was conducted using the first order conditional interaction estimation (FOCEI) method to allow for the consideration of both randomness in between-subject variability and variability in the residual error when predicting individual parameter values. Convergence criterion was

three significant digits. The selection of a model required a statistically significant improvement ($p<0.05$) in the NONMEM objective function value (OFV). The minimum value of the objection function (OFV [-2log-likelihood (-2LL)] provided by NONMEM serves as a guide during model building. Between nested models, $p<0.05$ equates to a reduction in the OBJ value by >3.84, based on a chi-square distribution with one degree of freedom. The selection of a model also required biologically plausible parameter estimates; these were informed by previous estimates from the available published literature discussed previously.

Error modelling is used to describe the variability in how well the data is described by the parameter Population parameter variability (PPV) was described using random effect variables ("ETA" or η), which were assumed to have a mean of 0 and a variance of (ω^2) which was estimated. An exponential error model was used for the random effect variables, which relates between-subject variability and the model parameters. An exponential error model assumes a log-normal distribution, and avoids the occurrence of parameter estimates falling below zero, or biologically plausible values.

$$\mathbf{P_i = P_{pop} \cdot e^{\eta individual}} \qquad \textbf{Equation 3.1}$$

Where P_i is the parameter of the individual and P_{pop} is the population parameter estimate for the parameter of interest P (e.g., CL and V).

Covariance between two elements of η, for example between clearance and volume of distribution, was used to derive their correlation (R)

$$\mathbf{R = covariance \Big/ \sqrt{\omega_{CL}^2 + \omega_V^2}} \qquad \textbf{Equation 3.2}$$

Observation model

An observational model such as a residual error model, aims to minimise the difference between observed and predicted values. A combined error model consisting of both proportional and additive residual error models was used to describe the residual unexplained variability (RUV) for the concentration predictions.

Allometric theory (see Chapter 1) was used to scale pharmacokinetic parameter estimates (CL and V) for size. Parameter estimates were standardized to a typical adult with a body weight (W) of 70kg using (Equation 3.3).

$$\mathbf{P_i = P_{STD} \times \left({W_i}/{70} \right)^{PWR}} \qquad \textbf{Equation 3.3}$$

Where W_i and P_i are the body weight and parameter value of the respective individual patient, P_{std} is the parameter value standardised to a 70kg individual, and PWR is the allometric exponent; ¾ for clearance and 1 for volume of distribution. The maturation of fentanyl clearance was described using a sigmoidal Hill function expressed as seen in (Equation 3.4). Age related changes in volume were also examined using a simple linear model seen in (Equation 3.5).

$$\mathbf{CL = CL_{std} \times \left(\frac{PMA^{Hill}}{PMA^{Hill} + TM_{50}^{Hill}} \right)} \qquad \textbf{Equation 3.4}$$

$$\mathbf{V = V_{std} \times (1 + slope \times \left(\frac{-PNA \times ln2}{TVOL} \right))} \qquad \textbf{Equation 3.5}$$

The quality of fit of the optimal model to the data was determined by visual examination of predictive checks (VPCs) (n of simulations = 1000) and observed versus predicted concentration plots. VPCs inform us on the appropriateness of the structural model in addition to the suitability of the error models, by graphically superimposing the optimal model simulations on the observations[56]. The 50th (median), 5th and 95th percentile predictions may be compared visually with those of the observations within these VPCs. Bootstrap methods (n=100) were also used to estimate the non-parametric confidence intervals of the parameter estimates as a measure of the uncertainty in the estimates [57, 58].

Shrinkage

In any mode, the quality of an individual's parameter estimate will depend on the observed data available. When data is scarce, the variance (ω^2) of parameter estimates can be reduced, along with distortion in the distribution shape of the data. If there were no data available for a subject, the

individuals estimate would be set equal to the population value; the variance shrinks towards zero as available data for a particular subject decrease, this occurrence is defined as η-shrinkage. Shrinkage (Shη%) is calculated using (Equation 3.6).

$$\mathbf{Sh_{\eta}\% = 100\ x\ \left\{1 - {SD(\eta)}/{\omega}\right\}} \qquad \textbf{Equation 3.6}$$

Where SD(η) is approximates the standard deviation of the random effects. A shrinkage of zero indicates the use of an appropriate model and that data availability on the individual level is sufficient for individual parameter estimation. A shrinkage of 100% indicates the data contains virtually no information about the parameter estimates and the individual parameter values approach the population parameter value.[59]

1-compartment

The first model to be investigated was 1 compartmental with first order elimination. This model was parameterised in terms of clearance (CL) and volume (V) from the sole compartment. These two parameter estimates were standardised using theory-based allometry to a 70kg individual. Age related changes in CL and V were also investigated and parameterised in this analysis. CONVD and TVOL are parameters used to describe the maturation changes of volume from neonates to adults as post-natal age (weeks) increases. Similarly, the parameters $TM_{50}CL$ and HILL describe the time it takes in post menstrual age (weeks) for the clearance of a neonate to reach 50% maturation of what it would be in an adult. The HILL parameter simply describes the slope of this maturation.

2-compartment

The second model to be investigated was 2 compartmental with first order elimination. This model was parameterised in terms of elimination clearance (CL) from the central compartment, inter-compartmental clearance (Q) between the central and peripheral compartment and volume of the central and peripheral compartments (V1, V2). These parameter estimates were standardised using theory-based allometry to a 70kg individual. Age related changes in CL, V1 and V2 were also investigated and parameterised in this analysis. CONVD1, CONVD2, TVOL1 and TVOL2 are parameters used to

describe the maturation changes of volumes in the central and peripheral compartments, from neonates to adults as post-natal age (weeks) increases. Similarly, the parameters $TM_{50}CL$ and HILL describe the time it takes in post menstrual age (weeks) for the clearance of a neonate to reach 50% maturation of what it would be in an adult. The HILL parameter simply describes the slope of this maturation.

3-compartment

The third model to be investigated was 3 compartmental with first order elimination. This model was parameterised in terms of elimination clearance (CL) from the central compartment, inter-compartmental clearance (Q2, Q3) between the central and peripheral compartments and volume of the central and peripheral compartments (V1, V2, V3). These parameter estimates were standardised using theory-based allometry to a 70kg individual. Age related changes in CL, V1, V2 and V3 were also investigated and parameterised in this analysis. CONVD1, CONVD2, CONVD3, TVOL1, TVOL2 and TVOL3 are parameters used to describe the maturation changes of volumes in the central and peripheral compartments, from neonates to adults as post-natal age (weeks) increases. Similarly, the parameters $TM_{50}CL$ and HILL describe the time it takes in post menstrual age (weeks) for the clearance of a neonate to reach 50% maturation of what it would be in an adult. The HILL parameter simply describes the slope of this maturation.

3.3 Results

Table 3.1: Patient characteristics for PK analysis. Data are presented as mean (range)

Participants	**N = 322/3016 (Subjects/Samples)**
PMA (weeks)	1866 (23.0 – 3690)
Weight (kg)	45.5 (0.49 – 130)

A total of 3016 observations in 322 subjects (182 paediatric, 140 adult) were available for the pooled analysis. Paediatric was deemed as $\leq$ 2 years of age. Characteristics of the pooled population are summarized within Table 3.1. Subjects had a mean (range) post-menstrual age of 1866 (26 – 3690) weeks and mean weight (range) of 45.5 (0.49 – 130) kg.

3.3.1 1-compartment

Observed concentrations from all individuals within the population are shown in Figure 3.1 and Figure 3.2 from a 1 compartment analysis. Observed concentrations plotted against individual concentrations based on population predictions (parameters only) notably stand out and are dispersed randomly compared to the line of identity in Figure 3.2. Observed concentrations plotted against individual Bayesian predictions (parameters + covariates) were more uniform however still slightly over predicted compared to the line of identity in Figure 3.1, reinforcing the influence of covariates on PK variability.

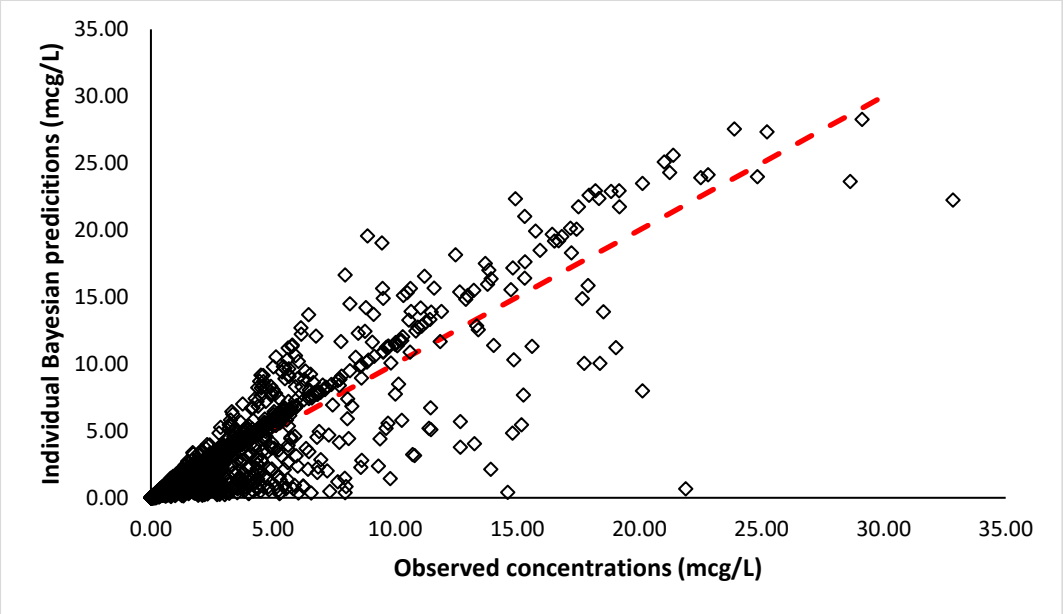

Figure 3.1: Comparison of individual Bayesian predicted and observed concentrations. Dotted shapes represent each individual. Dashed red line indicates the line of identity.

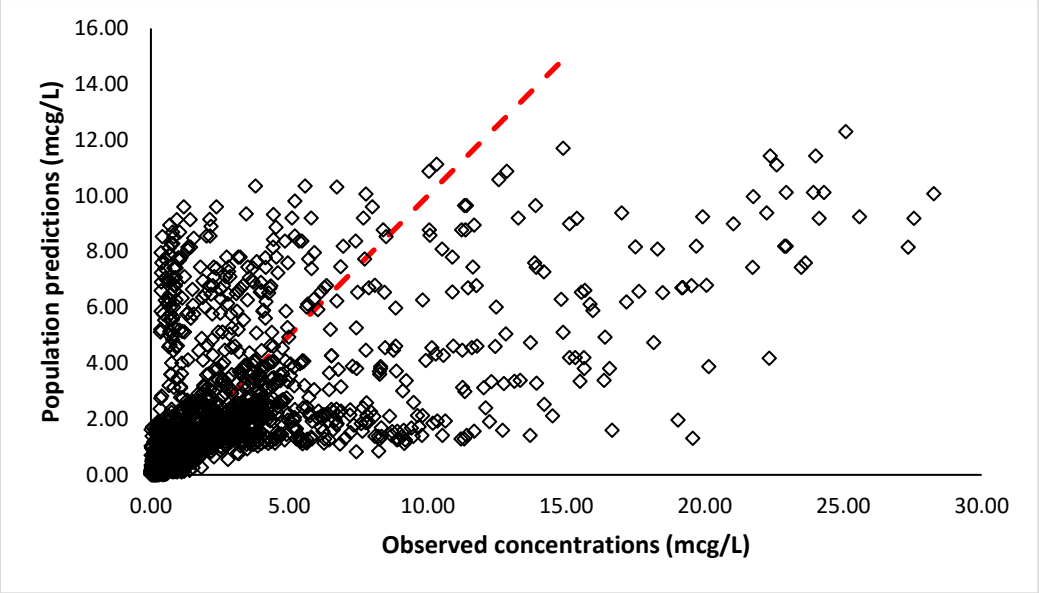

Figure 3.2: Comparison of population predicted and observed fentanyl concentrations. Dotted shapes represent each individual. Dashed red line represents the line of identity.

Table 3.2: Development of the one-compartment fentanyl population pharmacokinetic model. Changes in objective function value (OFV) are calculated relative to the models indicated by number.

No.	Model	Objective function value (OFV)	Compared to No.
1	No covariates	-2161.228	-
2	Allometric scaling for size	-2275.736 Δ -114.508	1
3	Allometric scaling for size and maturation function for CL	-2541.491 Δ -265.755	2
4	Allometric scaling for size, maturation function for CL and linear function for V	-2836.150 Δ -294.659	3

A decrease in the minimum value of the objective function value (Δ OFV) of 3.84 points from the base model when a parameter was added was considered significant at the 0.05 level. The factors of size and age on clearance and volume were added to the base model in a sequential process as shown above. The addition of size and age covariates to the one-compartment model significantly improved the model

through reduction of the OFV $\geq$ 3.84. NM-TRAN control stream for the final one-compartment model (Appendix 8).

Table 3.3: Fentanyl population pharmacokinetic parameter estimates for the final one compartment model. Population parameter variability presented as CV%, 95% CI represents the 95% confidence interval of the population parameter. Shr% represents the shrinkage.

Parameter	**Estimate**	**PPV (CV %)**	**95% CI**	**Shr%**
V (L/70kg)	62.6	79.3	52.1, 74.5	4.3
CL (L/min/70kg)	1.54	78.6	1.36, 1.74	5.0
CONVD	7.49	-	5.40, 9.27	-
TVOL	258	-	131.7, 413.2	-
$TM_{50}CL$	47.1	-	42.5, 58.2	-
Hill	3.52	-	2.72, 4.51	-

Volume of distribution V; clearance CL; $TM_{50}CL$ maturation half-time on CL; TVOL maturation half-time on V; CONVD describing steepness of volume maturation; Hill describing steepness of clearance maturation profile. Size accounted for using theory-based allometry, scaling to a standard 70kg individual with allometric exponents of ¾ for CL and 1 for V.

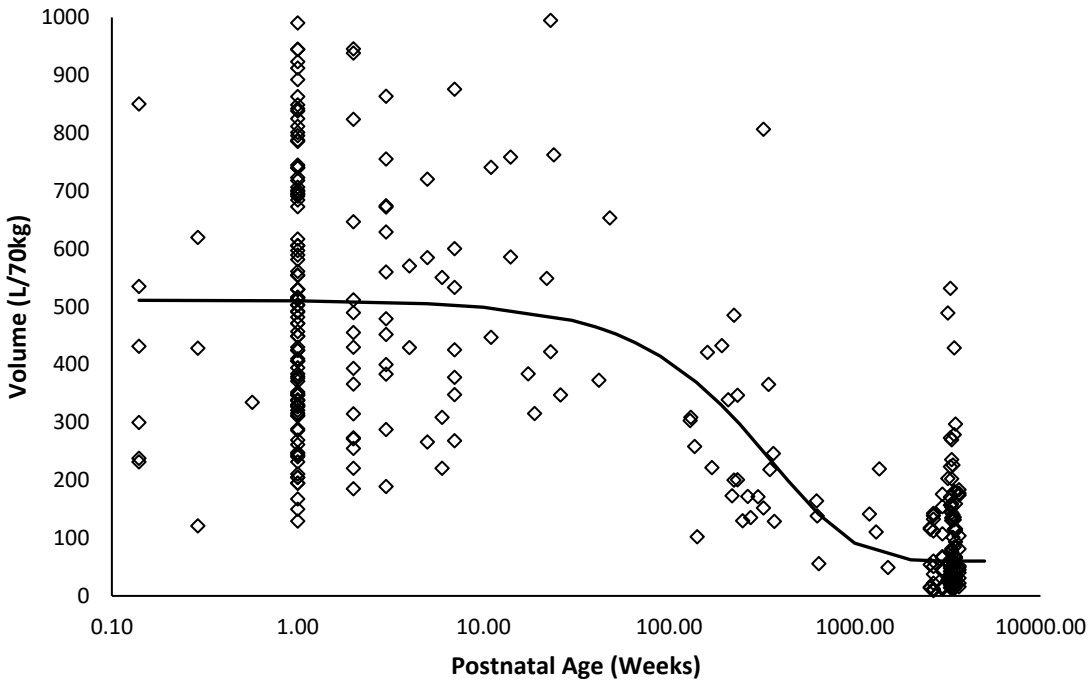

Figure 3.3: Maturation of fentanyl volume with post-natal age for each individual. Solid line represents population prediction. Changes in volume influenced by size, accounted for by allometric scaling of weight to a standardised 70kg individual

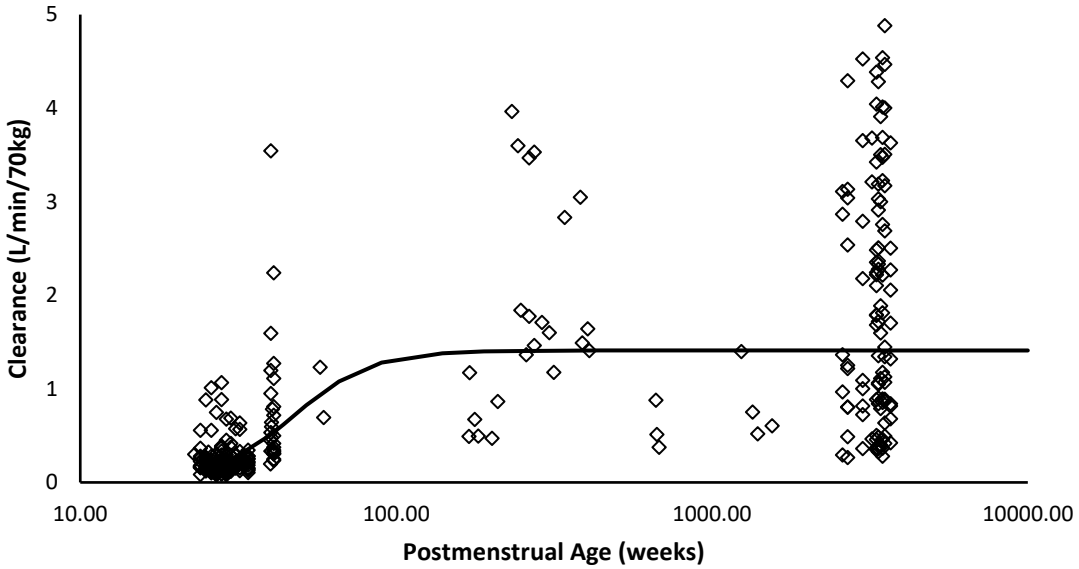

Figure 3.4: Maturation of fentanyl clearance with post-menstrual age for each individual. Solid line represents population prediction. Changes in clearance influenced by size, accounted for by allometric scaling of weight to a standardised 70kg individual

The volume of fentanyl is after one-compartmental analysis was higher within neonates and begins to decrease towards adult values at ~52 weeks PNA (1 year). Volume at birth was ~ 481 L/70kg and ~60 L/70kg in adults (see Figure 3.3). The clearance of fentanyl is lower within neonates and reaches close to adult values after ~90 weeks PMA (1 year of age). Clearance at 26 weeks PMA was ~0.16 L/min/70kg and ~1.40 L/min/70kg in adults (see Figure 3.4)

The ratio of between subject variability predictable from covariates ($BSVP^2$) to the total population parameter variability estimated without covariate analysis ($PPVt^2$), provides information on the impact of covariate effects (see Table 3.4).

Table 3.4: Impact of covariance analysis on variance (ω^2) of clearance and volume when each covariate is added sequentially to the final model.

Model	**$PPVt^2$**	**$BSVR^2$**	**$BSVP^2$**	**$BSVP^2$ / $PPVt^2$**
Clearance				
CL no covariates	6.750	6.750	0	0
Allometric scaling of body size on CL	6.750	1.490	5.260	0.780
PMA + Allometry on CL	6.750	0.746	6.004	0.889
Volume				
Volume no covariates	1.680	1.440	0	0
Allometric scaling of body size on V	1.680	1.440	0.240	0.143
PNA + Allometry on V	1.680	0.629	1.051	0.625

88.9% of variability associated with CL is explained by allometric scaling of size and a postmenstrual age sigmoidal function on maturation (Equation 3.3 and Equation 3.4). 62.5% of variability associated with V is explained by allometric scaling of size and a postnatal age linear function (Equation 3.3 and Equation 3.5).

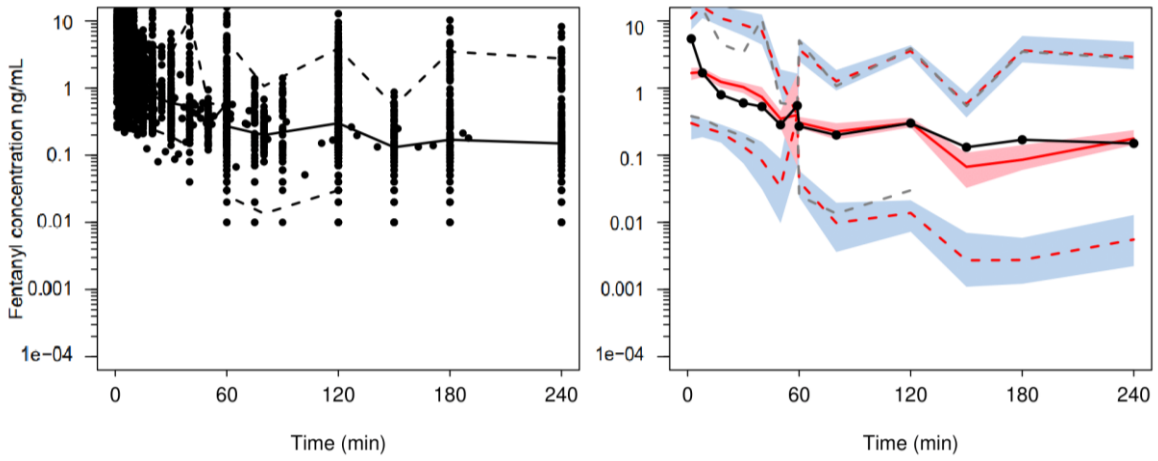

Figure 3.5: Visual predictive check for the final one-compartment pharmacokinetic model. All plots shows median (solid lines) and 90% intervals (dashed lines). The plot of the left shows the observed fentanyl concentrations. The plot on the right shows the 10^{th}, 50^{th} and 90^{th} percentiles for the predictions (red-dashed lines) overlaid with the 10^{th}, 50^{th} and 90^{th} percentiles for the observations (grey-dashed line). The blue shaded areas represent the 95% confidence intervals for the prediction percentiles.

The visual predictive check seen in Figure 3.5 shows that the predicted and observed concentrations of fentanyl from 0 to 60 minutes are slightly overpredicted by the model. The model also appears to overpredict underpredict the concentration of fentanyl from 120 to 240 minutes. Prediction of the early fentanyl concentration could be fixed by introducing a secondary compartment to the model.

3.3.2 2-compartment

Observed concentrations from all individuals within the population are shown in Figure 3.6 and Figure 3.7 from a 2-compartment analysis. Observed concentrations plotted against individual concentrations based on population predictions (parameters only) notably stand out from the line of identity in Figure 3.6. Observed concentrations plotted against individual Bayesian predictions (parameters + covariates) tightly fit along the line of identity in Figure 3.7, visualising how much pharmacokinetic variability in fentanyl concentrations is explained by covariates within this model.

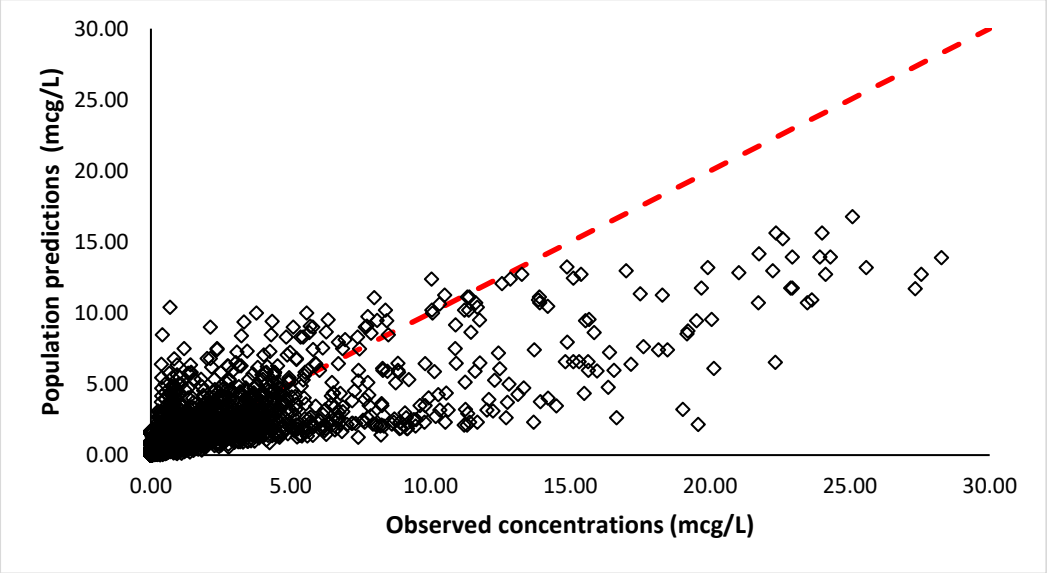

Figure 3.6: Comparison of population predicted and observed fentanyl concentrations. Dotted shapes represent each individual. Dashed red line represents the line of identity.

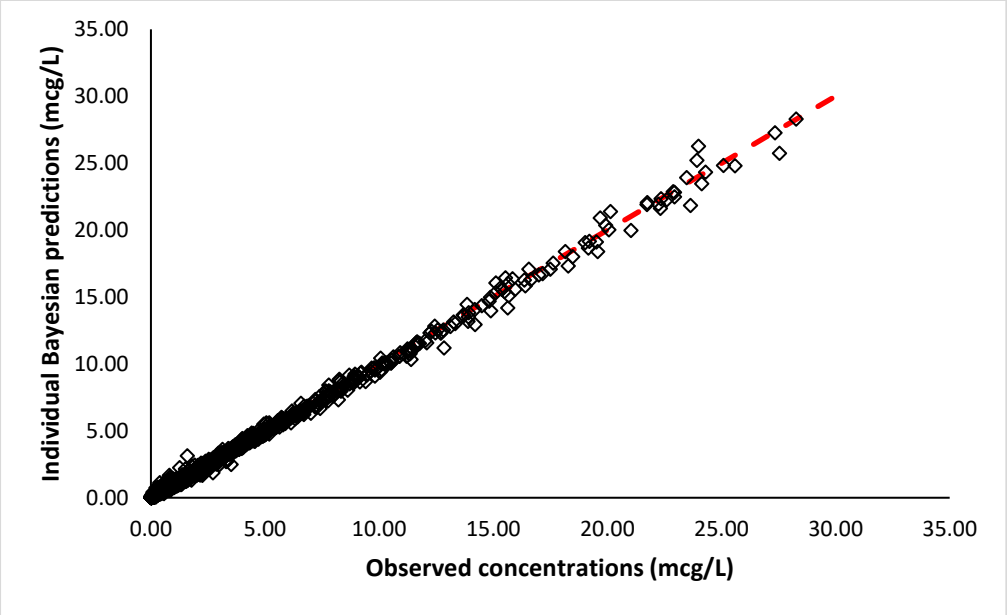

Figure 3.7: Comparison of individual Bayesian predicted and observed concentrations. Dotted shapes represent each individual. Dashed red line indicates the line of identity.

Table 3.5: Development of the two-compartment fentanyl population pharmacokinetic model. Changes in objective function value (OFV) are calculated relative to the nested models indicated by number.

No.	Model	Objective function value (OFV)	Compared to No.
1	No covariates	-5378.179	-
2	Allometric scaling for size	-5946.053 Δ -567.874	1
3	Allometric scaling for size and maturation function for CL	-6174.870 Δ -228.817	2
4	Allometric scaling for size, maturation function for CL and linear function for V1	-6374.353 Δ -199.483	3
5	Allometric scaling for size, maturation function for CL and linear function for V1 and V2	-6400.277 Δ -225.407	3

A decrease in the minimum value of the objective function value (Δ OFV) of 3.84 points from the base model when a parameter was added was considered significant at the 0.05 level. The factors of size and age on clearance and volume were added to the base model in a sequential process as shown above. The addition of size and age covariates to the two-compartment model significantly improved the model through reduction of the OFV $\geq$ 3.84. NM-TRAN control stream for the final two-compartment model (Appendix 9)

Table 3.6: Fentanyl population pharmacokinetic parameter estimates for the final two compartment model. Population parameter variability presented as CV%, 95% CI represents the 95% confidence interval of the population parameter. Shr% represents the shrinkage.

Parameter	Estimate	PPV (CV %)	95% CI	Shr%
V1 (L/70kg)	36.4	104.4	28.2, 43.0	7.6
V2 (L/70kg)	96.7	119.6	76.5, 104.6	22.9
CL (L/min/70kg)	1.41	68.1	1.28, 1.59	5.0
Q (L/min/70kg)	3.22	144.9	2.78, 4.21	28.9
CONVD1	8.36	-	6.30, 10.2	-
CONVD2	0.776	-	0.694, 1.76	-
TVOL1	237	-	224, 458	-
TVOL2	2.28	-	1.84, 5.1	-
$TM_{50}CL$	45.3	-	42.8, 49,6	-
Hill	4.11	-	3.36, 4.59	-

Central compartment volume of distribution V1; peripheral compartment volume of distribution V2; clearance CL; inter-compartmental clearance Q; $TM_{50}CL$ maturation half-time on CL; TVOL1 and TVOL2 maturation half-time on V1 and V2; CONVD1 and CONVD2 describing steepness of V1 and V2 maturation; Hill describing steepness of clearance maturation profile. Size accounted for using theory-based allometry, scaling to a standard 70kg individual with allometric exponents of ¾ for CL and 1 for V.

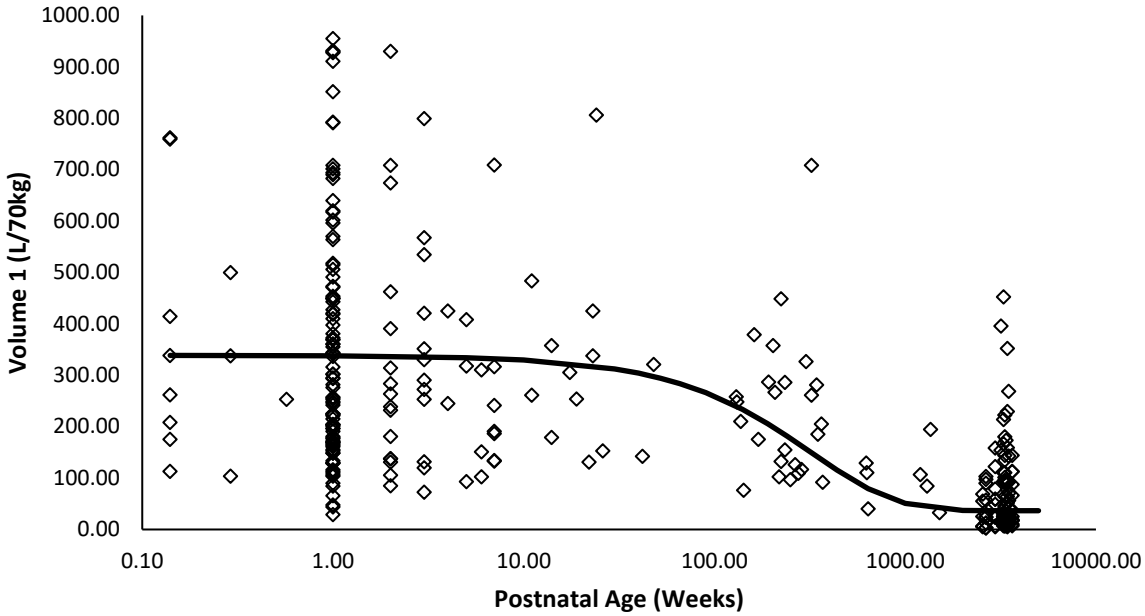

Figure 3.8: Maturation of central compartment fentanyl volume with post-natal age for each individual. Solid line represents population prediction. Changes in volume influenced by size, accounted for by allometric scaling of weight to a standardised 70kg individual

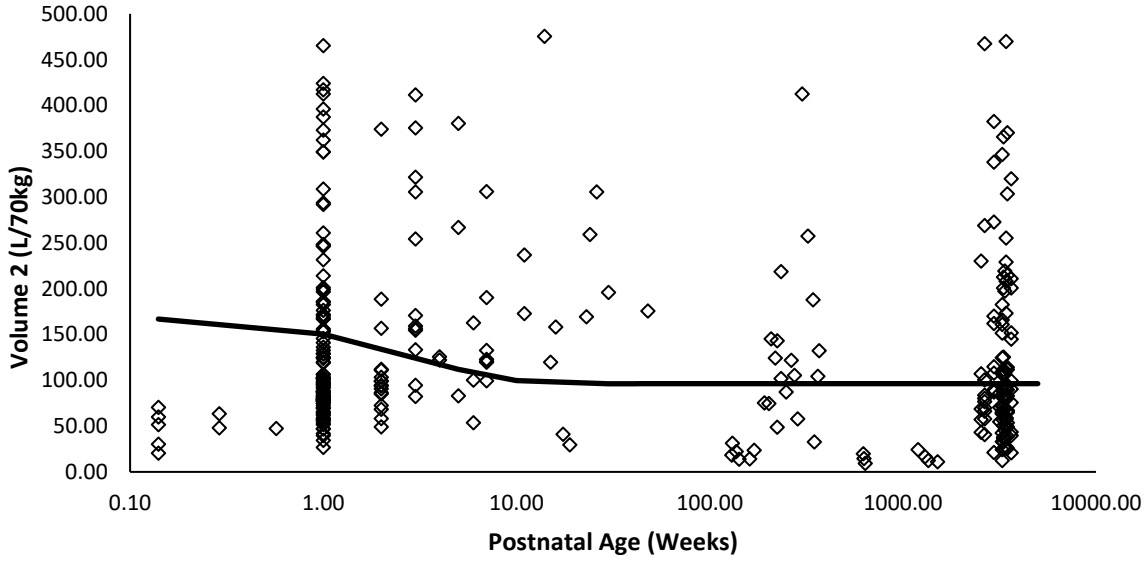

Figure 3.9: Maturation of peripheral compartment fentanyl volume with post-natal age for each individual. Solid line represents population prediction. Changes in volume influenced by size, accounted for by allometric scaling of weight to a standardised 70kg individual

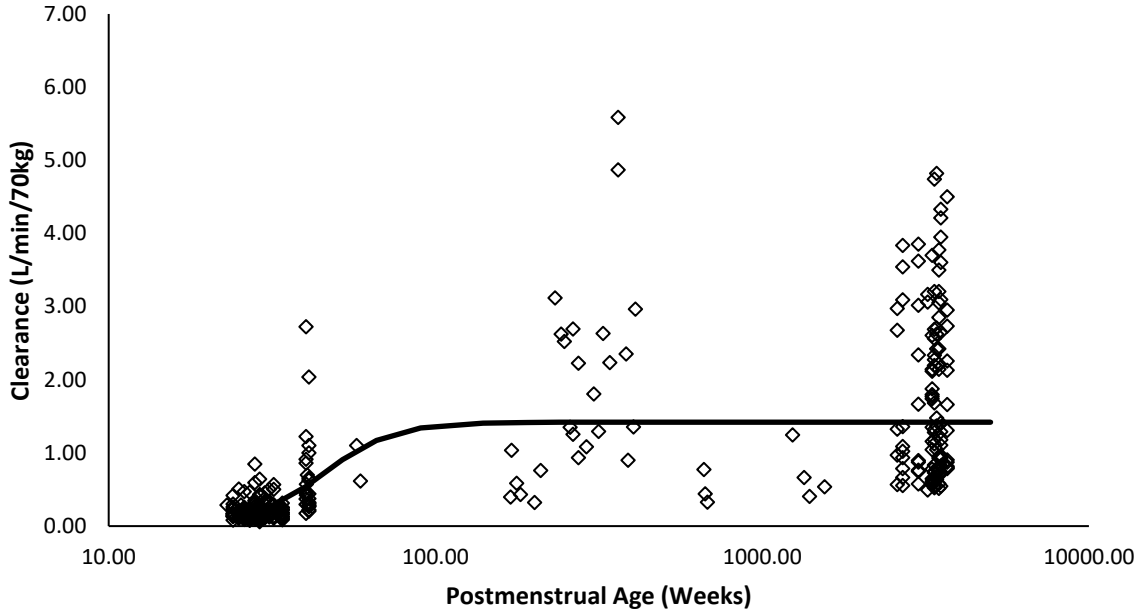

Figure 3.10: Maturation of fentanyl clearance with post-menstrual age for each individual. Solid line represents population prediction. Changes in clearance influenced by size, accounted for by allometric scaling of weight to a standardised 70kg individual

The central and peripheral compartment volumes of fentanyl after the two-compartmental analysis was higher within neonates and begins to decrease towards adult values at ~40 weeks PNA for the central compartment, and at ~5 weeks PNA for the peripheral compartment. Central compartment volume at birth was ~ 337 L/70kg and ~37 L/70kg in adults (see Figure 3.8). Peripheral compartment volume at birth was ~ 166 L/70kg and ~96 L/70kg in adults (see Figure 3.9). The clearance of fentanyl is lower within neonates and reaches close to adult values after ~90 weeks PMA (1 year of age). Clearance at 26 weeks PMA was ~0.14 L/min/70kg and ~1.41 L/min/70kg in adults (see Figure 3.10)

Table 3.7: Impact of covariance analysis on variance (ω^2) of clearance and volumes when each covariate is added sequentially to the final model.

Model	**PPVt^2**	**BSVR^2**	**BSVP^2**	**BSVP^2 / PPVt^2**
Clearance				
CL no covariates	6.740	6.740	0	0
Allometric scaling of body size on CL	6.740	1.700	5.040	0.747
PMA + Allometry on CL	6.740	0.432	6.308	0.935
Volume 1				
V1 no covariates	1.750	1.750	0	0
Allometric scaling of body size on V1	1.750	1.710	0.040	0.023
PNA + Allometry on V1	1.750	0.973	0.777	0.444
Volume 2				
V2 no covariates	3.240	3.240	0	0
Allometric scaling of body size on V2	3.240	1.320	1.920	0.593
PNA + Allometry on V2	3.240	1.196	2.044	0.631

93.5% of variability associated with CL is explained by allometric scaling of size and a postmenstrual age sigmoidal function on maturation (Equation 3.3 and Equation 3.4). 44.4% and 63.1% of variability associated with V1 and V2 is explained by allometric scaling of size and a postnatal age linear function (Equation 3.3 and Equation 3.5).

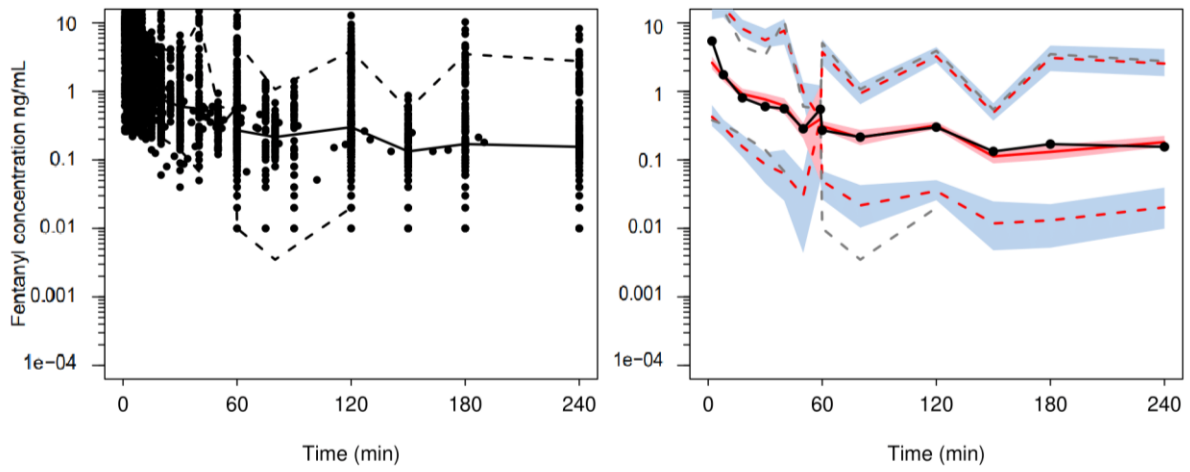

Figure 3.11: Visual predictive check for the final two-compartment pharmacokinetic model. All plots show median (solid lines) and 90% intervals (dashed lines). The plot of the left shows the observed fentanyl concentrations. The plot on the right shows the 10th, 50th and 90th percentiles for the predictions (red-dashed lines) overlaid with the 10th, 50th and 90th percentiles for the observations (grey-dashed line). The blue shaded areas represent the 95% confidence intervals for the prediction percentiles.

The visual predictive check seen in Figure 3.11 shows that the predicted and observed concentrations of fentanyl from 0 to 240 minutes are very similar to one another and fit tightly against one another. The model appears to overpredict the 90th percentile concentration at show around the 60 – 120 minutes when compared to the observed values. This could be attributed to the observed values reaching such low concentrations around this time point, which would make predictions at this point difficult.

3.3.3 3-compartment

Observed concentrations from all individuals within the population are shown in Figure 3.12 and Figure 3.13 from a 3-compartment analysis. Observed concentrations plotted against individual concentrations based on population predictions (parameters only) notably stand out and are under predicted based on the line of identity in Figure 3.12. Observed concentrations plotted against individual Bayesian predictions (parameters + covariates) tightly fit along the line of identity in Figure 3.13, visualising how much pharmacokinetic variability in fentanyl concentrations is explained by covariates within this 3-compartment model.

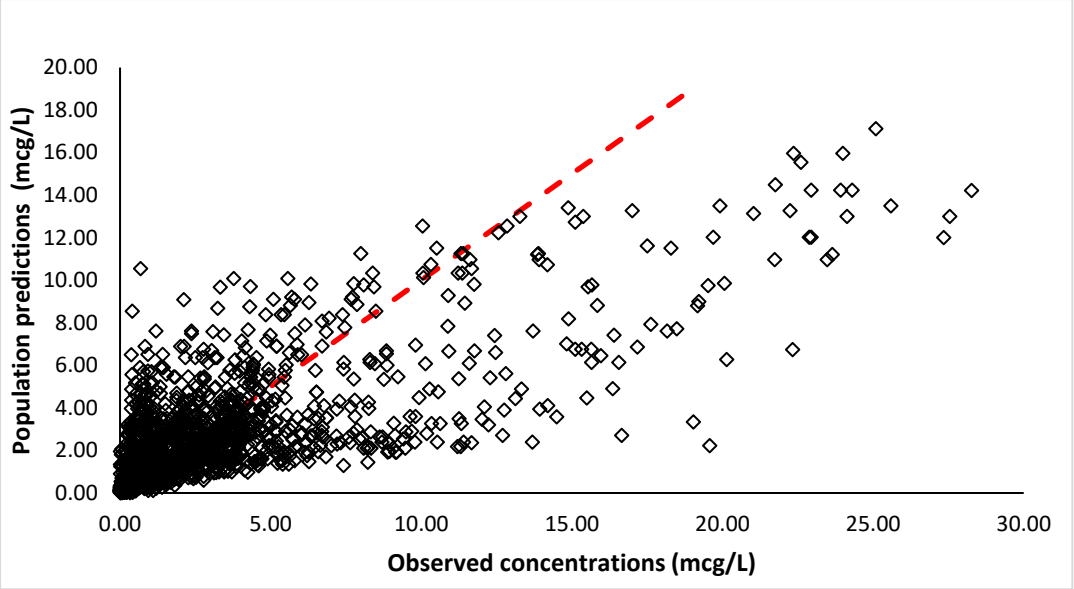

Figure 3.12: Comparison of population predicted and observed fentanyl concentrations. Dotted shapes represent each individual. Dashed red line represents the line of identity.

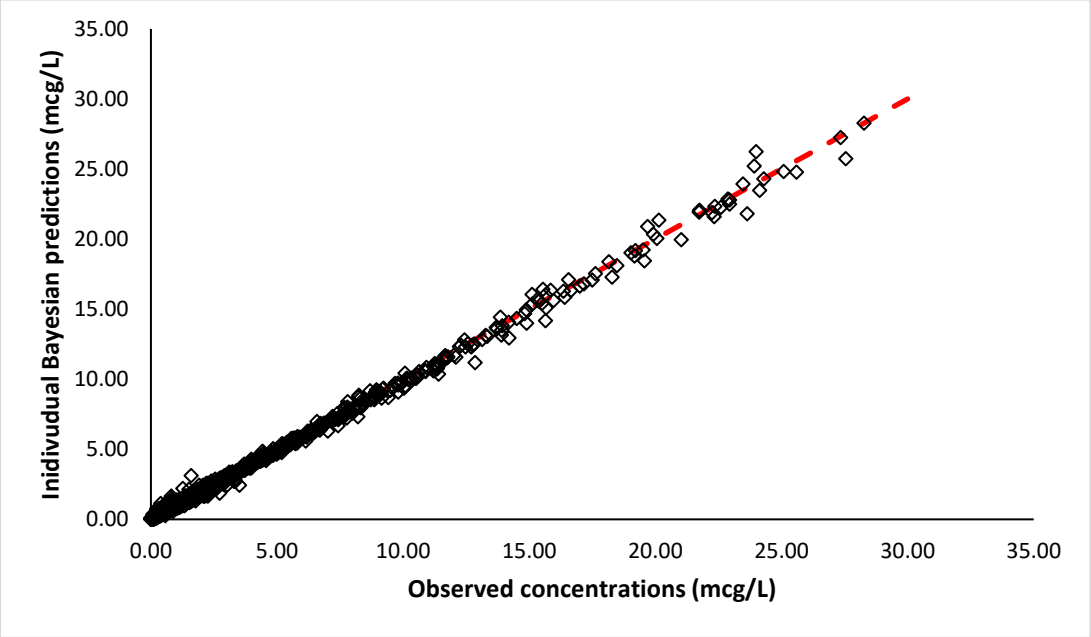

Figure 3.13: Comparison of individual Bayesian predicted and observed concentrations. Dotted shapes represent each individual. Dashed red line indicates the line of identity.

Table 3.8: Development of the three-compartment fentanyl population pharmacokinetic model. Changes in objective function value (OFV) are calculated relative to the models indicated by number.

No.	Model	Objective function value (OFV)	Compared to No.
1	No covariates	-5569.770	-
2	Allometric scaling for size	-6055.357 Δ -485.587	1
3	Allometric scaling for size and maturation function for CL	-6190.977 Δ -135.620	2
4	Allometric scaling for size, maturation function for CL and linear function for V1	-6383.120 Δ -192.143	3
5	Allometric scaling for size, maturation function for CL and linear function for V1 and V2	-6386.598 Δ -195.621	3
6	Allometric scaling for size, maturation function for CL and linear function for V1, V2 and V3	-6427.060 Δ -236.083	3

A decrease in the minimum value of the objective function value (Δ OFV) of 3.84 points from the base model when a parameter was added was considered significant at the 0.05 level. The factors of size and age on clearance and volume were added to the base model in a sequential process as shown above. The addition of size and age covariates to the two-compartment model significantly improved the model through reduction of the OFV $\geq$ 3.84. NM-TRAN control stream for the final three-compartment model (Appendix 10)

Table 3.9: Fentanyl population pharmacokinetic parameter estimates for the final three-compartment model. Population parameter variability presented as CV%, 95% CI represents the 95% confidence interval of the population parameter. Shr% represents the shrinkage.

Parameter	Estimate	PPV (CV %)	95% CI	Shr%
V1 (L/70kg)	35.1	104.4	31.9, 43.2	9.1
V2 (L/70kg)	82.1	139.6	73.1, 91.2	25.7
V3 (L/70kg)	509	80.6	404, 587	26.3
CL (L/min/70kg)	1.29	85.3	1.19, 1.45	8.9
Q2 (L/min/70kg)	3.43	144.6	3.09, 4.52	29.4
Q3 (L/min/70kg)	0.0518	159.1	0.0424, 0.0704	40.7
CONVD1	8.37	-	6.33, 9.13	-
CONVD2	0.692	-	0.513, 0.936	-
CONVD3	0.492	-	0.241, 0.543	-
TVOL1	208	-	203, 388	-
TVOL2	13.9	-	7.29, 16.0	-
TVOL3	58	-	47.0, 114	-
$TM_{50}CL$	51.4	-	48.5, 52.6	-
Hill	3.58	-	3.40, 4.17	-

Central compartment volume of distribution V1 ; peripheral compartments volume of distribution V2 and V3 clearance CL; inter-compartmental clearance between central and peripheral compartment Q2; inter-compartmental clearance between both peripheral compartments Q3; $TM_{50}CL$ maturation half-time on CL; TVOL1, TVOL2 and TVOL3 maturation half-time on V1, V2 and V3; CONVD1 , CONVD2 and CONVD 3 describing steepness of V1, V2 and V3 maturation ; Hill describing steepness of clearance maturation profile. Size accounted for using theory-based allometry, scaling to a standard 70kg individual with allometric exponents of ¾ for CL and 1 for V.

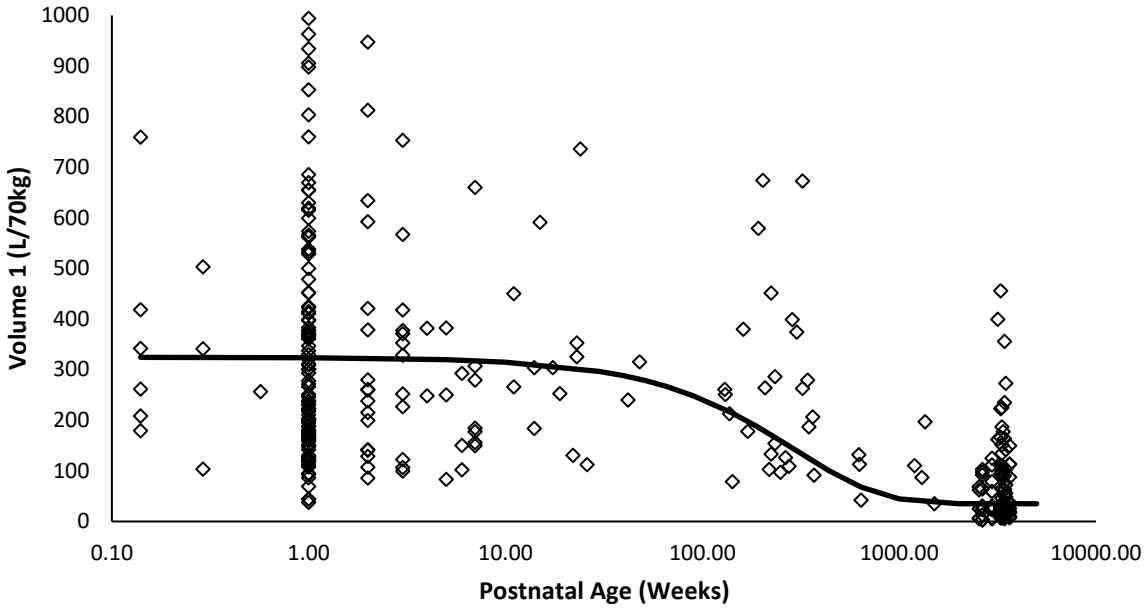

Figure 3.14: Maturation of central compartment fentanyl volume with post-natal age for each individual. Solid line represents population prediction. Changes in volume influenced by size, accounted for by allometric scaling of weight to a standardised 70kg individual

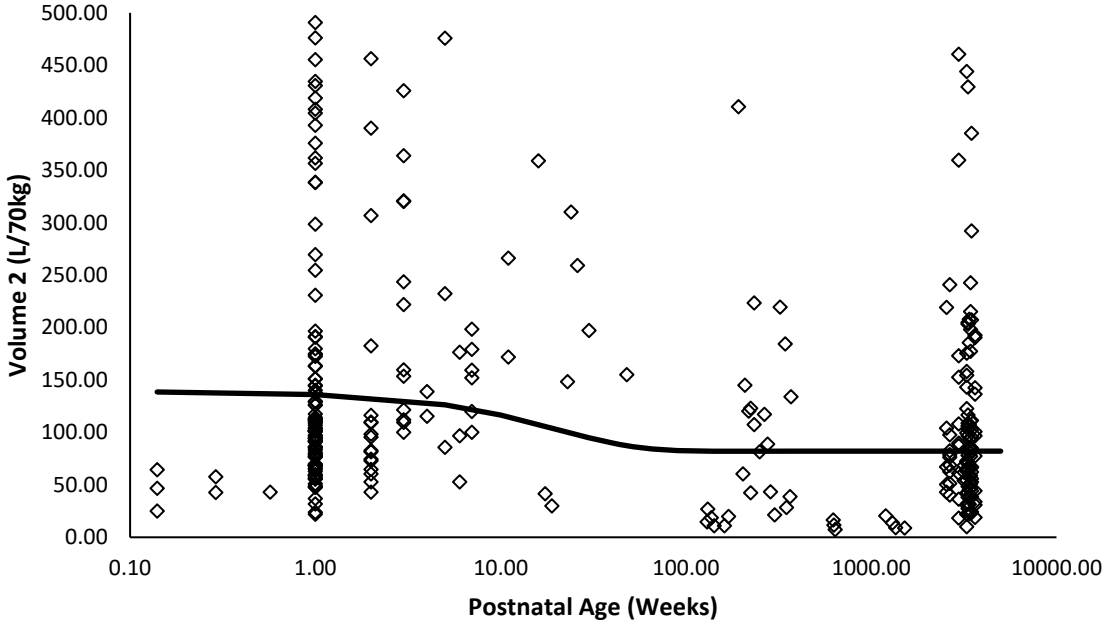

Figure 3.15: Maturation of peripheral compartment fentanyl volume with post-natal age for each individual. Solid line represents population prediction. Changes in volume influenced by size, accounted for by allometric scaling of weight to a standardised 70kg individual

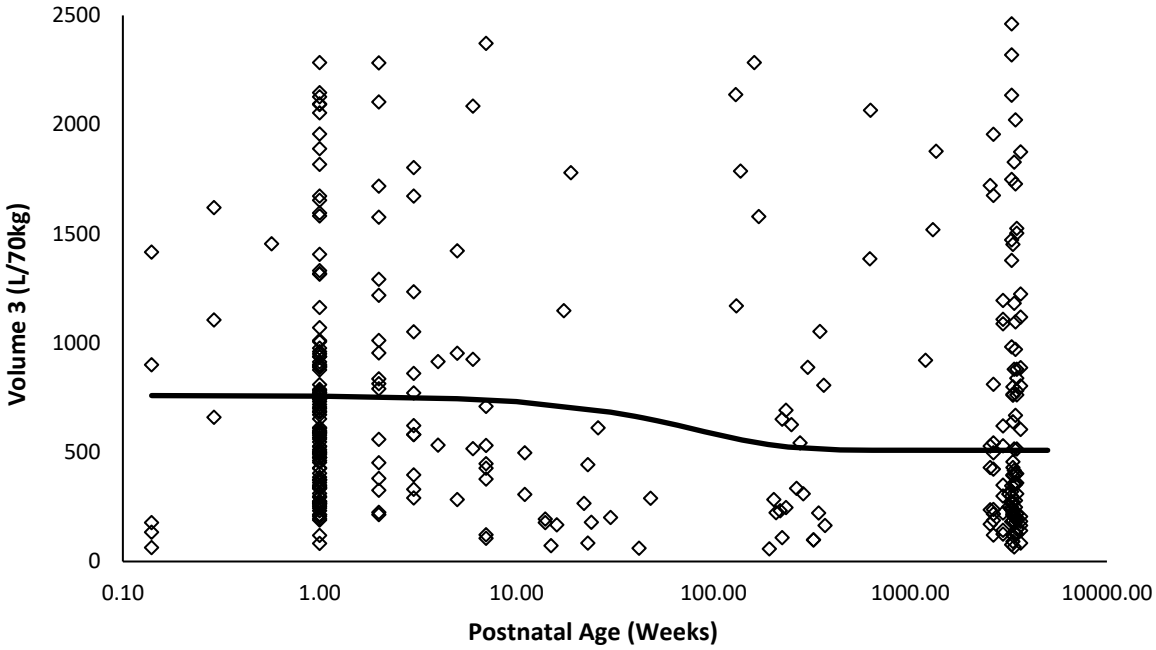

Figure 3.16: Maturation of peripheral compartment fentanyl volume with post-natal age for each individual. Solid line represents population prediction. Changes in volume influenced by size, accounted for by allometric scaling of weight to a standardised 70kg individual

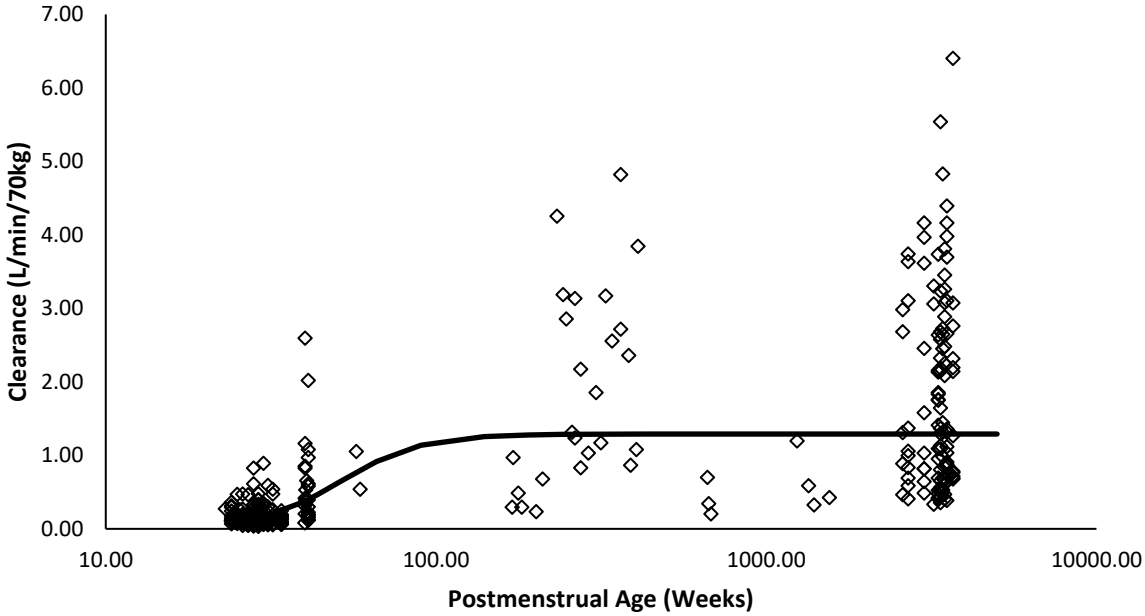

Figure 3.17: Maturation of fentanyl clearance with post-menstrual age for each individual. Solid line represents population prediction. Changes in clearance influenced by size, accounted for by allometric scaling of weight to a standardised 70kg individual

The central and peripheral compartment volumes of fentanyl after the three-compartmental analysis was higher within neonates and begins to decrease towards adult values at ~40 weeks PNA for the central compartment (V1), ~5 weeks PNA for the peripheral compartment (V2) and ~1-week PNA for the peripheral compartment (V3). Central compartment volume (V1) at birth was ~323 L/70kg and ~35 L/70kg in adults (see Figure 3.14). Peripheral compartment volume (V2) at birth was ~138 L/70kg and ~82 L/70kg in adults (see Figure 3.15). Peripheral compartment volume (V3) at birth was ~750 L/70kg and ~509L/70kg in adults (see Figure 3.16). The clearance of fentanyl is lower within neonates and reaches close to adult values after ~90 weeks PMA (1 year of age). Clearance at 26 weeks PMA was ~0.11 L/min/70kg and ~1.29 L/min/70kg in adults (see Figure 3.17).

Table 3.10: Impact of covariance analysis on variance (ω^2) of clearance and volumes when each covariate is added sequentially to the final model.

Model	**PPVt^2**	**BSVR^2**	**BSVP^2**	**BSVP^2 / PPVt^2**
Clearance				
CL no covariates	6.140	6.140	0	0
Allometric scaling of body size on CL	6.140	0.812	5.328	0.867
PMA + Allometry on CL	6.140	0.504	5.636	0.918
Volume 1				
V1 no covariates	2.270	2.270	0	0
Allometric scaling of body size on V1	2.270	2.211	0.059	0.026
PNA + Allometry on V1	2.270	1.220	1.050	0.463
Volume 2				
V2 no covariates	6.280	6.280	0	0
Allometric scaling of body size on V2	6.280	4.050	2.23	0.355
PNA + Allometry on V2	6.280	2.010	4.270	0.679
Volume 3				
V3 no covariates	18.20	18.20	0	0
Allometric scaling of body size on V3	18.20	0.649	17.55	0.964
PNA + Allometry on V3	18.20	0.518	17.68	0.971

91.8% of variability associated with CL is explained by allometric scaling of size and a postmenstrual age sigmoidal function on maturation (Equation 3.3 and Equation 3.4). 46.3%, 67.9% and 97.1% of variability associated with V1, V2 and V3 is explained by allometric scaling of size and a postnatal age linear function (Equation 3.3 and Equation 3.5).

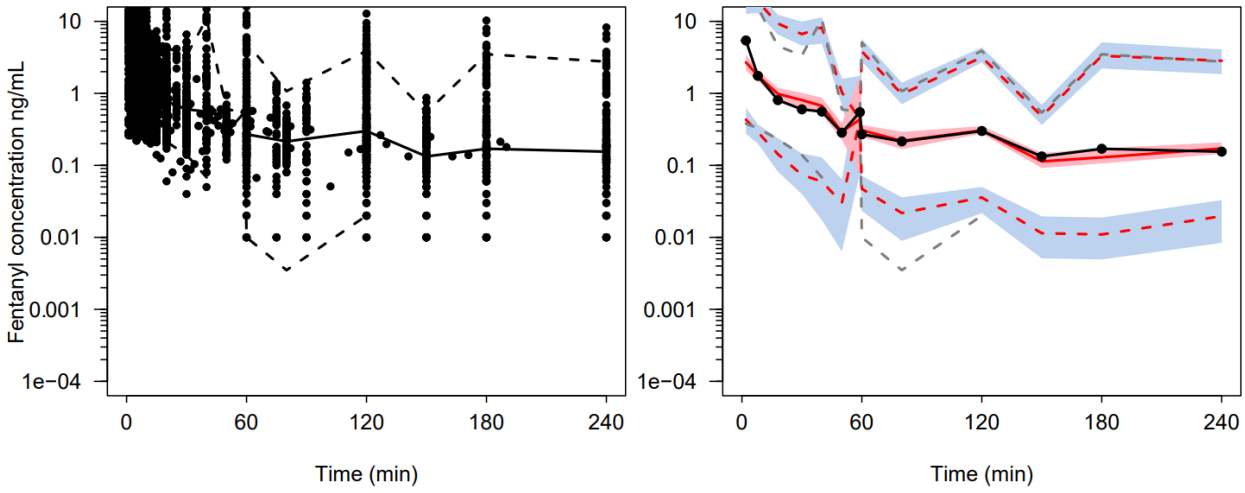

Figure 3.18: Visual predictive check for the final three-compartment pharmacokinetic model. All plots shows median (solid lines) and 90% intervals (dashed lines). The plot of the left shows the observed fentanyl concentrations. The plot on the right shows the 10th, 50th and 90th percentiles for the predictions (red-dashed lines) overlaid with the 10th, 50th and 90th percentiles for the observations (grey-dashed line). The blue shaded areas represent the 95% confidence intervals for the prediction percentiles.

Estimated population parameters and their variability for this model are shown in Table 3.9. The maturation of fentanyl clearance is visualized in Figure 3.17 when standardised to a typical 70kg body weight using allometry. The maturation profile of fentanyl clearance was described by a $TM_{50}CL$ of 51.4 weeks and a HILL slope of 3.58 (see Table 3.9). Clearance values reached 90% of mature size standardized adult values at 90 weeks post-menstrual age, which is equivalent to ~1-year post-natal age. The relationship between volume of distribution and age was described for each of the compartments in this model. The relationship between central compartment volume (V1) and age was estimated to have a slope 8.31 and described by a TVOL1 of 208 weeks (see Table 3.9). The maturation profile of V1 is depicted in Figure 3.14. The relationship between both peripheral compartment volumes (V2 and V3) and age was not as profound as it was for V1, with slope estimation of 0.692 and 0.493 for V2 and V3 respectively (see Figure 3.15 and Figure 3.16).

The final three-compartment model significantly reduced the OFV (-3590.91 points and -45 points, $p \leq 0.05$), compared to the final one-compartment and two-compartment model respectively (See Table 3.2, Table 3.5 and Table 3.8). The large delta in OFV between the final one-compartment and three-

compartment model informed the decision to no longer pursue the one-compartment model in the selection for the final model. To further justify this choice, the individual predictions for observed fentanyl concentrations were scattered and less uniform from the one-compartment model (see Figure 3.1), compared to the two and three compartment models (see Figure 3.7 and Figure 3.13).

3.4 Discussion

Comparing the results of the final three-compartment model to the two-compartment model, both models were capable of individually predicting fentanyl concentrations from the observed values, with Figure 3.7 and Figure 3.13 both appearing similarly in goodness of fit along the line of identity. As mentioned prior, the final three-compartment model did improve upon the OFV of the two-compartment model by a significant value (-45 points, $p \leq 0.05$), which does inform model selection. An analysis of covariance was conducted for each of the final models, which provided empirical evidence on the impact of the covariates when added to each of the parameters in a step-wise process. Both models showed that the addition of the size and age covariates, contributed for 70-80% of the overall variability in clearance (see Table 3.7 and Table 3.10). This, in addition to the largest significant reduction in OFV lead to the three-compartment model being selected as the best model for the fentanyl population pharmacokinetic data.

A three-compartment pharmacokinetic model with allometric scaling for clearance and volume parameters, a maturation function to account for clearance changes with age, and linear functions to account for all three volume of distribution changes age, generated the best model fit to describe the fentanyl population pharmacokinetic data. Age and size were important covariates added to describe the variability associated to clearance and volume within the population. Simulating time-concentration data from multiple studies and pooling this, allowed for the ability investigate covariates across a wide range of ages (preterm neonates to adults) within a single pharmacokinetic analysis. Fentanyl is metabolised by CYP3A4-mediated N-dealkylation to the inactive metabolite norfentanyl [60]. The activity of CYP3A4 was not evaluated within this study. The maturation of clearance, which was

investigated, coincides with the maturation of the metabolic enzymes responsible for the elimination of fentanyl (CYP3A4) [61].

Size and age covariates were shown to be important covariates in the pharmacokinetics of fentanyl, and contributed to 91.8% of the population variability in clearance. The impact of size on fentanyl pharmacokinetics was investigated with total body weight (TBW) scaled using allometric scaling. TBW represents the most commonly used weight indicator and coupled with allometric scaling, is proven to be the most suitable size scalar for fentanyl clearance [62, 63]. Post-menstrual age was the most appropriate descriptor of maturation in this analysis, as studies have proven clearance maturation processes begin well before birth (in utero) [38, 53]. Previous studies have described how size and age related changes alter the clearance of an individual, and have shown that size and age are the primary descriptors of predicting fentanyl clearance from premature neonates to children (24 weeks to 300 weeks PMA; 0 to 5+ years of age) [50, 54, 61]. The allometric scaling of clearance to a fully mature 70kg adult was used to investigate these age-related changes of fentanyl clearance, using a sigmoidal maturation function independent of size, which was utilised within this analysis. The estimate of adult standardised clearance in this study (1.29 L/h/70kg; 85.3 CV%; 95% CI 1.19, 1.45) was similar to other clearance estimates reported by Foster et al (1.23 L/h/70kg; 22.0 CV%; 95% CI 1.04, 1.39) and Loughren et al (0.96 L/h/70kg; 95% CI 0.73, 1.21) [49, 50]. Furthermore the estimate of clearance from this analysis is within the range of values reported within previous fentanyl pharmacokinetic analyses in children and adults (0.4 - 1.8 L/h/70kg) [35, 43, 46, 50, 51]. The maturation profile of fentanyl clearance in this analysis was estimated and described by maturation half-life (51.4 weeks PMA; 95% CI 48.5, 52.6) and HILL slope (3.58; 95% CI 3.40, 4.17) (see Table 3.9). These estimates from this analysis were similar to those described in neonates, infants and children by others for midazolam (73.6 weeks PMA; 95% CI 59.4, 80.0; 3.00 95% CI 2.20, 4.10) [64]. Fentanyl and midazolam share similar maturation profiles as they are both primarily mediated by CYP3A4 metabolism. The authors noted that the midazolam maturation appeared to be delayed in this study, compared to other drugs cleared by CYP3A4 (fentanyl) [64]. This was due to a lack of midazolam estimates in neonates aged 40-88 weeks PMA, which is crucial information needed for describing maturation in the early stages of infancy [64]. In vitro studies suggest CYP3A4 activity reaches

30-40% of adult activity after 4 weeks PMA, and reaches close to adult values ~1 year after birth [65, 66]. This data from literature is like results from this analysis, which found clearance reaching 90% of mature size-standardized adult values at 90 weeks post-menstrual age, which is equivalent to ~1-year post-natal age (See Figure 3.17). These differences in maturation times from this analysis compared to literature can be attributed to secondary elimination pathways of fentanyl. Evidence suggests although fentanyl elimination is primarily through metabolism, ~15-20% of elimination can be attributed to excretion through the kidneys [67].

Size and age covariates were shown to be important covariates in relation to the volume of distribution of fentanyl, and contributed to 46.3%, 67.9% and 97.1% of the population variability in V1, V2 and V3 respectively. Similar to clearance, allometry coupled with TBW was the most suitable size descriptor for volume in this analysis [68, 69]. Post-natal age was the most appropriate descriptor of maturation for volume in this analysis, as evidence shows volume changes only begin to occur after birth [53]. Previous studies have described how size and age related difference influence the volume of an individual, and are primary descriptors for predicting fentanyl's volume in neonates to adults (0 – 20 + years of age) [42, 70]. Allometric scaling of volume to a fully mature 70kg standardised individual was used to investigate the age-related changes of fentanyl volume, along with a maturation function independent of size. The estimate of adult standardised volumes in this study; V1 (35.1 L/70kg; 104.4 CV%; 95% CI 31.9, 43.2), V2 (82.1 L/70kg; 139.6 CV%; 95% CI 73.1, 91.2), V3 (509 L/70kg; 80.6 CV%; 95% CI 404, 587), were similar to other volumes estimated by others V1 (10-60 L/70kg), V2 (65 -150 L/70kg), V3 (250 – 600 L/70kg) [20, 46, 48, 49, 53]. The wide ranges of volume estimates from other studies, when compared to estimates from this analysis could be attributed to studies not including a maturation function for volume, as was done in this analysis. The maturation function used in this analysis, incorporated an equation to account age-related changes which influence the volume of distribution for fentanyl (See Equation 3.5). Large differences in V3 estimates when comparing this analysis to other studies can be associated to the scarcity of 3-compartmental analysis involving fentanyl within literature. The maturation profile of fentanyl volume in each of the compartments in this analysis was estimated and described using a linear model, with maturation half-life (TVOL) and slope (CONVD) for each

compartment; V1 (208 weeks PNA; 95% CI 203, 388; 8.37; 95% CI 6.33, 9.13), V2 (13.9 weeks PNA; 95% CI 7.29, 16.0; 0.692; 95% CI 0.513, 0.939), V3 (58.0 weeks PNA; 95% CI 47.0, 114; 0.492; 95% CI 0.241, 0.543). Volume was shown to be at its highest within neonates, remaining mostly constant for the first ~40 weeks PNA, before decreasing over time until adulthood. This most likely explained by the fact neonates and especially preterm neonates have a lower percentage of fat and muscle in proportion to weight, when compared to adults [42]. Fentanyl is highly lipophilic and redistributes heavily into fat and muscle, resulting in the increased volume of distribution within neonates seen in the maturation of volume in this analysis (see Figure 3.14, Figure 3.15 and Figure 3.16) [70].

A visual predictive check (VPC) illustrates the model's appropriateness for the observed fentanyl concentrations and compares this to what the model predicts the concentration should be. The visual predictive check seen in Figure 3.18 shows that the model heavily under-predicts fentanyl concentrations at around the 60 to 120 minutes post administration. This could be attributed to the observed values reaching such low concentrations around this time point, which would make predictions at this point difficult.

3.5 Conclusion

The work presented in this chapter strengthens the importance of age and size covariates when modelling the pharmacokinetics of fentanyl within individuals aged from premature neonates to adults. The clearance of fentanyl was shown to increase with age, rapidly maturing within the first few months of infancy, and coincides with the ontogeny of the processes that are primarily responsible for the metabolism of fentanyl. Fentanyl's volume of distribution was largest in neonates, and decreased slowly towards adults' values 1 year after birth. This is most likely attributed to maturational changes in body composition, lower proportions of fat and muscle in respect to weight, and the high lipophilicity of fentanyl.

4 Intranasal and Oral Fentanyl absorption characteristics

4.1 Introduction + aims

Intranasal fentanyl bypasses the oral/gastrointestinal route and has proven to be useful in cancer patients experiencing nausea, vomiting, oral mucositis, and gastrointestinal function [11]. Intranasal fentanyl has a bioavailability of 89% with a short onset of action of ~5-20 minutes [11]. Intranasal fentanyl spray multi dose was approved in 2009 under the brand name Instanyl® [71]. In 2011 a single dose INFS spray, using the same formulation was also approved. INFS delivers a small dose (20 to 100ug) of fentanyl within the nasal cavity, with similar pH of the nasal mucosa to avoid local irritation [11]. The oral route of administration for fentanyl is another delivery method for children, due to its non-invasive nature. Oral transmucosal fentanyl (Fentanyl Oralet) was approved by the FDA for premedication of children but is no longer marketed, due to high incidence of vomiting as an adverse effect and reports of misuse for personal reasons by staff [72, 73]. A new formulation (Actiq) has been approved for adults and children 16 years of age or older, but it has been used off-label in children for the treatment of cancer breakthrough pain.[74-76] This route of administration provides more rapid onset of analgesia than buccal immediate-release tablets (5-10 minutes) but is slower in onset than nasal administration (2.4 minutes) [76]. Fentanyl is rapidly absorbed through the oral mucosa, which undergoes first pass metabolism [76-84]. Nonetheless, approximately half the absorption is gastrointestinal. Consequently, the bioavailability of this formulation in children (33%) is less than that in adults (50%) [83, 84]. Uptake continues for a period of time after consumption, which potentially can provide analgesia for several hours [82-84].

The aims of this chapter were to

a) Simulate concentration-time profiles consisting of neonatal to adult subjects from existing nasal and Fentanyl Oralet studies
b) Carry over the 3-compartment population model from previous chapter produces and estimate the parameters Tabs, TLag and F to describe the absorption characteristics of fentanyl within this population

4.2 Literature search

Pharmacokinetic studies involving fentanyl use conducted in children were identified from a literature search in PubMed, using the following search terms and key words to identify the most appropriate studies: Intranasal fentanyl, Oral fentanyl, Intranasal PK, Pharmacokinetics, PK, Absorption parameters, Population modelling, Children, Neonate(s), Paediatric(s), Infant(s), Review, Postnatal, Preterm, Population, Analysis, Modelling.

Data collated from the literature was formatted in such a way that was suitable for analysis through the NONMEM software

a). Identification of PK absorption parameter values Tabs, Tlag and F from the literature review, for children between the ages of 0-18 years. An attempt to use papers which defined absorption parameters for individuals was done. However, not all papers provide individual data and other studies simply define mean values for the entire study cohort. An excel spreadsheet from this was created and included parameters estimates (CL and V), absorption parameters (Tabs, Tlag and F) weight (kg), age and, formulation (oral or nasal)

b) Literature parameter values reported for CL, V and absorption parameters were used to simulate individuals and create time-concentration profiles in subjects (premature neonates to adolescents).

c) Time-concentration profiles for individuals or naïve pooled analysis groups, when available in literature, was also added to the simulated data

d) Paediatric studies which provided absorption parameter estimates were not available within literature, simulation of paediatric intranasal/oral fentanyl data was not possible

d) All demographic information from studies involving nasal fentanyl administration were collated into a table for simulation

e) Raw concentration from a study involving Fentanyl Oralet was provided by Wheeler et al, which was used in the analysis step

Table 4.1: Published literature estimates of fentanyl's absorption parameters within individuals. Data is all from studies involving intranasal administration of fentanyl

Study	Patients (n)	PMA (weeks)	Weight (kg)	Tabs (min)	Tlag (minutes)	F (fraction)
Foster et al[48]	24	2588-3680	58-130	3.41	1.08	1
	24	-	-	6.41	5.20	0.89
	24	-	-	6.93	3.00	0.80
Valtola et al[85]	16	2548-3640	55-125	1.86	3.00	0.765
Lim et al[51]	8	1444-3264	52-90	2.66	0	0.55
	11	-	-	3.15	0	0.71

4.3 Simulation of data

Simulation of the individual concentration data using non-linear mixed effect modelling (NONMEM 7.4, ICON Development Solutions, Hanover, MD, USA). Simulations were conducted using the Monte Carto method and followed similar methods to what was done previously for the IV fentanyl simulations (See Methods). A total of 3 studies involving intranasal fentanyl PK analysis were found from the literature search. Demographic information from the 3 studies used for this simulation (see Table 4.1), were pooled and resampled to create a simulation data file. The demographic information for each patient included; age, weight, post-menstrual age, post-natal age, and gestational age. The studies used for this simulation only included adult, paediatric data was not available. The age range of subjects across the 3 studies was (27 to 70 years of age). Simulating adult concentration data from studies involving intranasal administration was important for the estimation of PK absorption parameters. Fentanyl concentrations were simulated at time points like what was previously done in each study, as the aim was to emulate each studies concentration profiles. All fentanyl concentration measurements were taken after administration. Fentanyl concentrations were simulated at time points ranged between 0 and 300 minutes. The administration of fentanyl in these studies included intranasal single bolus doses (50 – 200ug).

Pharmacokinetic information was published within each of the 3 studies used, which was used in the simulation of fentanyl concentration time data. The studies included in the simulation were a variety of 1, 2 and 3 compartmental analyses. The pharmacokinetic information of interest from these studies were the absorption parameters Tabs, Tlag and F. All 3 studies provided these absorption parameter estimates along with the required compartmental parameters CL and V, as well as additional parameters V2, Q1, V3 and Q2 for the 2 and 3 compartmental studies. Some studies provided an estimate of the absorption rate constant (ka) parameter instead of a Tabs estimate, in these scenarios Equation 4.1 was used to convert.

$$\boldsymbol{Tabs = \frac{\ln(2)}{Ka}} \qquad \textbf{Equation 4.1}$$

Table 4.2: Final combined simulation data from all 3 studies

Participants	**N = 107/1112 (Subjects/Samples)**
PMA (weeks)	2746 (1444 – 3690)
Weight (kg)	66.75 (52 – 130)

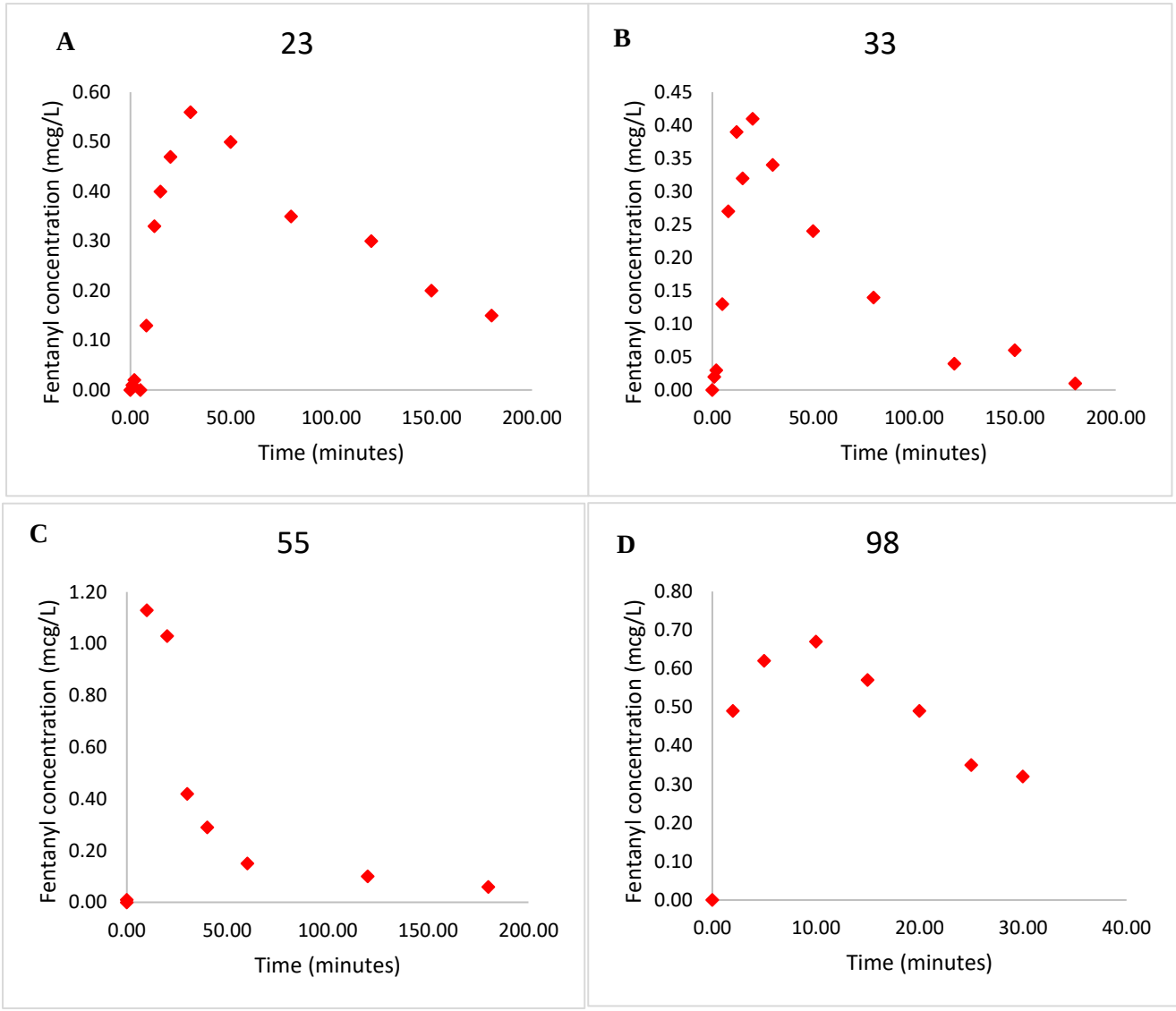

Figure 4.1: Individual concentration time profiles of subjects 23, 33, 55 and 98, simulated by NONMEM. **A:** 63 year old patient received 100ug intranasal dose, **B;** 64 year old received a 100ug intranasal dose, **C;** 70 year old received a 200ug intranasal dose, **D;** 56 year old received a 50ug intranasal dose.

4.4 PK analysis Methods

Non-linear mixed effect models were constructed and used for the pharmacokinetic analysis of intravenous fentanyl. Model building for non-linear mixed effects involves the process of determining the characteristics for both the fixed and random effects of a population, while still managing to include individual differences within that population. Analysis of the individual PK data using non-linear mixed effect modelling (NONMEM 7.4, ICON Development Solutions, Hanover, MD, USA). NONMEM is used to define the population distribution of PK absorption parameters (Tabs, Tlag and F) through estimation of the population characteristics. Methods for the PK analysis within this chapter mimic what was done for the IV analysis of fentanyl (See Methods).

This analysis used the time-concentration data which was simulated from intranasal fentanyl dosing information, collected from the literature review (See Table 4.1). These simulated time-concentration profiles only consisted of adult population data, as paediatric intranasal fentanyl PK data was not available. A study by Wheeler et al was found, which investigated the pharmacokinetics of Fentanyl Oralet in children [84]. Fentanyl Oralet is an oral transmucosal drug delivery system which provides a painless method of delivering fentanyl to the patient, and is acceptable for use within children. Per request, the authors provided the plasma fentanyl raw concentration data from the patients taking Fentanyl Oralet. This resulted in 38 individual child patient profiles being added to the combined simulated patient data file. With the addition of these data, it was possible to analyse and estimate the PK of Fentanyl Oralet and intranasal fentanyl within the same model.

Model selection for this PK analysis of oral + nasal fentanyl was based off the final model selected for the analysis of IV data (see Appendix 10). The PK estimates; CL, V1, V2, V3, Q2, Q3 and maturation functions for CL and V were all fixed within the final model, as these estimated prior and to stabilise the estimation for the absorption parameters of interest. The final model included equations for the estimation of both oral and nasal parameter estimates, these were defined as TABPO, LAG and FPO for oral absorption parameters, and TABN, LAGN and FN for nasal absorption parameters. The NM-TRAN control file for the final model can be seen in Appendix 11.

4.5 Results

A total of 1470 observations in 145 subjects were available for the pooled analysis. Characteristics of the pooled population are summarized within Table 4.3. Subjects had a mean (range) post-menstrual age of 2473 (218 – 3680) weeks and mean weight (range) of 66.75 (13.5 – 130) kg.

Table 4.3: Patient characteristics for PK analysis. Data are presented as mean (range)

Participants	**N = 145/1470 (Subjects/Samples)**
PMA (weeks)	2473 (218 – 3680)
Weight (kg)	66.75 (13.5 – 130)

Goodness of fit plots for observed fentanyl concentration compared to population predicted and individual Bayesian predicted concentrations of fentanyl for a combined model with all IV, nasal and oral data are provided within the appendices (Appendix 12 and Appendix 13). A visual predictive check of this final model is also provided within the appendices (Appendix 14).

Table 4.4: Fentanyl population pharmacokinetic parameter estimates for the final three-compartment model intranasal and oral model. Population parameter variability is presented as a percentage (PPV %), 95% CI represents the 95% confidence interval of the population parameter. Shr% represents the shrinkage.

Parameter	Estimate	PPV (CV %)	95% CI	Shr%
V2 (L/70kg)	35.1	104.4	31.9, 43.2	9.1
V3 (L/70kg)	82.1	139.6	73.1, 91.2	25.7
V4 (L/70kg)	509	80.6	404, 587	26.3
CL (L/min/70kg)	1.29	85.3	1.19, 1.45	8.9
Q3 (L/min/70kg)	3.43	144.6	3.09, 4.52	29.4
Q4 (L/min/70kg)	0.0518	159.1	0.0424, 0.0704	40.7
Tabs nasal (min^{-1})	7.69	257.9	6.85, 9.68	85.9
TLag nasal (min)	2.59	45.8	2.11, 2.94	52.5
F nasal (fraction)	0.94	-	0.89, 0.94	-
Tabs oral (min^{-1})	7.45	240.1	6.83, 15.4	83.5
TLag oral (min)	6.00	46.8	5.51, 7.21	82.2
F oral (fraction)	0.42	-	0.35, 0.45	-
CONVD2	8.37	-	6.33, 9.13	-
CONVD3	0.692	-	0.513, 0.936	-
CONVD4	0.492	-	0.241, 0.543	-
TVOL2	208	-	203, 388	-
TVOL3	13.9	-	7.29, 16.0	-
TVOL4	58	-	47.0, 114	-
$TM_{50}CL$	51.4	-	48.5, 52.6	-
Hill	3.58	-	3.40, 4.17	-

Central compartment volume of distribution V2 ; peripheral compartments volume of distribution V3 and V4 clearance CL; inter-compartmental clearance between central and peripheral compartment Q3; inter-compartmental clearance between both peripheral compartments Q4; $TM_{50}CL$ maturation half-time on CL; TVOL2, TVOL3 and TVOL4 maturation half-time on V2, V3 and V4; CONVD2 , CONVD3 and CONVD4 describing steepness of V2, V3 and V4 maturation ; Hill describing steepness of clearance maturation profile. Absorption half-life, lag time and bioavailability for nasal fentanyl Tabs nasal, TLag nasal and F nasal; Absorption half-life, lag time and bioavailability for Fentanyl Oralet Tabs oral, TLag oral and F oral. Size accounted for using theory-based allometry, scaling to a standard 70kg individual with allometric exponents of ¾ for CL and 1 for V.

4.6 Discussion

Absorption parameters estimated for nasal fentanyl; Tabs (7.69; 259 CV%; 95% CI 6.85, 9.68) and TLag (2.59; 45.0 CV%; 95% CI 2.11, 2.94) were similar to those previously estimated by Upton et al; Tabs (4.36; 53.9 CV%) and Tlag (2.23; 53.9 CV%) [86]. The bioavailability of nasal fentanyl estimated in this analysis F (0.904, 95% CI 0.89, 0.94) is well within the range of values provided by other available analyses F (0.771 – 0.940) [11, 48, 87]. Absorption parameters estimated for Fentanyl Oralet; Tabs (7.45; 240.1 CV%; 95% CI 6.83, 15.4) and TLag (6.00; 46.8 CV%; 95% CI 5.51, 7.21) were noticeably different to those previously estimated by other studies Tabs (6.30– 13.1) and Tlag (5.1 – 13.0) [88, 89]. The bioavailability of Fentanyl Oralet estimated in this analysis F (0.42, 95% CI 0.35, 0.45) is within the range of estimates from other studies F (0.35 – 0.55) [11, 77, 80, 90]. The coefficient of variation for the absorption half-life of both nasal and Fentanyl Oralet were notably high at 259% and 240% respectively, indicating a greater dispersion of data for this estimate than expected. An explanation for this could be the lack of concentration samples for both nasal and Fentanyl Oralet, resulting in a mean which is less likely to follow a normal distribution. The 95% confidence interval for the Fentanyl Oralet absorption half-life and bioavailability were larger than what was observed for the nasal estimates. This could be attributed to the limitations involved in using an oral transmucosal delivery method for a drug, such as ;enzymatic degradation, taste, limited surface area, poor tissue penetration and accidental swallowing [91]. There was a limited amount of data and a small pool of patients for both the nasal and Fentanyl Oralet formulations (107 nasal and 38 oral) patients. All subjects involved with the nasal data were from adults, while the Fentanyl Oralet data only consisted of children aged 3-10 years of age. Incorporation of more paediatric data, specifically neonates and infants ($\leq$ 2 years of age) for both nasal and Fentanyl Oralet formulations of fentanyl could add to future analyses and aid in describing changes in absorption half-life, lag time and bioavailability with age.

5 Conclusions

Understanding fentanyl pharmacokinetics in paediatrics is important for improving management of pain and clinical outcome of this population. This thesis contributes to the knowledge on fentanyl pharmacokinetics and how these change with age. The models reported within this analysis can be used to predict the clearance and volume of fentanyl form neonates to adults, which is useful for informing dose selection. Furthermore, a model for the pharmacokinetics of non-intravenous fentanyl formulations, nasal and Fentanyl Oralet is reported within this analysis. Further work is also needed within this space, particularly involving a pharmacodynamics-based model to describe the concentration-effect relationship of fentanyl, however this model is the first step for individualising the dosing of fentanyl through target concentration intervention. Additionally, more information for fentanyl absorption pharmacokinetics in the paediatric population, particularly neonates is required for further analysis to inform dosing using these formulations.

6 List of Appendices

Appendix 1: NM-TRAN code for a 2-compartment population pharmacokinetic model used for simulation of Study 1

```
$PROB SIM Fentanyl Wu infant.2 cmt

$DATA fentanyl_Wu_infant_2cmt.csv IGNORE #

$INPUT ID TIME AMT RATE DUR DV MDV DVID PNA GA PMA WT BW ASY SEX

$SIM (1751957 NEW) ONLYSIM SUB=1

; Wu Y. Pre- and Postnatal Maturation are Important for Fentanyl Exposure in
Preterm and Term Newborns: A Pooled Population Pharmacokinetic Study Clin
Pharmacokinet 2022, 61, 401-412

; units conc = mcg/L, BW = g, PNA = days, time =h, infusion mcg/h GA = weeks,
ASY= study 1 or 2



$THETA (0.0001,0.00525, 50)      ; TVCL

$THETA (0.001,14, 100)      ; TVV1

$THETA (0.0001,0.00596,50)       ; TVQ

$THETA (0.1,3.37,20)           ; TVV2



$THETA  1.47                ; PWR

$THETA  0.495               ; FPNA

$THETA  1.54                ; L1

$THETA  0.44               ; M1



;Residual unidentified variability

; separate errors for each study
```

```
; Study 1 Saarenmaa E, Neuvonen PJ, Fellman V. Gestational age and birth
weight effects on plasma clearance of fentanyl in newborn infants.J Pediatr.
2000;136(6):767–70

; Study 2 Völler S, Flint RB, Andriessen P, Allegaert K, Zimmermann LJI,
Liem KD, et al. Rapidly maturing fentanyl clearance in preterm neonates.
Arch Dis Child Fetal Neonatal Ed. 2019;104(6):F598


$THETA (0,0.253,) ; RUV_SDCP1

$THETA (0,0.226,) ; RUV_CVCP1

$THETA (0,0.0285,) ; RUV_SDCP2

$THETA (0,0.367,) ; RUV_CVCP2


$OMEGA 0.2   ; PPVCL

$OMEGA 0.207 ; PPVV1

$OMEGA 0 FIX  ; PPVQ

$OMEGA 0 FIX ; PPVV2


;Residual Unidentified Variability (Observations)

$OMEGA 0 FIX ; PPV_RUVCP1

$OMEGA 0 FIX ; PPV_RUVCP2


; residual error

$SIGMA 1. FIX ; EPS1


$SUBR ADVAN3 TRANS4

$PK

IF (NEWIND.LE.1) THEN    ; sets dose to 0 when start new patient
```

```
   LN2=LOG(2)
   DOSE=0                ; gives doses in output
 ENDIF

 ;PMA = PNA/7 + GA

   SZCL = (BW/1055)**PWR
   SZPNA = (PNA+0.01)**FPNA
   BDE = L1 * (WT/1165)**M1
   SZV = (WT/1165)**BDE

   CL=TVCL*SZCL * SZPNA *EXP(PPVCL)
   V1=TVV1* SZV *EXP(PPVV1)
   Q =TVQ*EXP(PPVQ)
   V2=TVV2*EXP(PPVV2)

  S1=V1

 $ERROR
  CP=A(1)/S1

 IF (ASY.EQ.1) THEN
  PROP1=CP*RUV_CVCP1
  ADD1=RUV_SDCP1
  SDCP=SQRT(PROP1*PROP1 + ADD1*ADD1)*EXP(PPV_RUVCP1)
ELSE
```

```
  PROP1=0
  ADD1=0
  SDCP=0
ENDIF
IF (ASY.EQ.2) THEN
  PROP2=CP*RUV_CVCP2
  ADD2=RUV_SDCP2
  SDCP=SQRT(PROP2*PROP2 + ADD2*ADD2)*EXP(PPV_RUVCP2)
ELSE
  PROP2=0
  ADD2=0
  SDCP=0
ENDIF

Y=CP + SDCP*EPS1

$TABLE ID TIME WT CL V1 Q V2 Y MDV PNA GA
ONEHEADER NOPRINT FILE=fentanyl.fit
```

Appendix 2: NM-TRAN code for a 1-compartment population pharmacokinetic model used for simulation of Study 2

```
-----------------------------------------------------------------------------------------------------------------

$PROB SIM Fentanyl children 1day1 Koehntop cmt

$DATA fentanyl_Koehntop_child_1day1_1cmt.csv IGNORE #

$INPUT ID TIME AMT DUR RATE CMT OCC MDV DVID DV AGE WT HT SEX FORM PNA PMA
GEST

$SIM (1234567 NEW) ONLYSIM SUB=1

; Koehntop DE, Rodman JH, Brundage DM, Hegland MG, Buckley JJ.
Pharmacokinetics of fentanyl in neonates. Anesthesia & Analgesia.
1986;65(3):227-32.


$THETA (0.01,0.0858,100)      ; CL

$THETA (1,8.61,200)        ; V


;Residual unidentified variability

$THETA 0 FIX ; RUV_SDCP

$THETA 0 FIX ; RUV_CVCP


$OMEGA 0.3  ; PPVCL

$OMEGA 0.2  ; PPVV


;Residual Unidentified Variability (Observations)

$OMEGA 0 FIX ; PPV_RUVCP


; residual error

$SIGMA 1. FIX ; EPS1


$SUBR ADVAN1 TRANS2
```

```
$PK
IF (NEWIND.LE.1) THEN    ; sets dose to 0 when start new patient
   LN2=LOG(2)
   DOSE=0                ; gives doses in output
 ENDIF

   FSZV= 1;WT/70
   FSZCL= 1; FSZV**0.75
   FSZT= 1;FSZV**0.25

   CL=FSZCL*CL*EXP(PPVCL)

   V=FSZV*V*EXP(PPVV)

 $ERROR

  CP=A(1)/V

 PROP=CP*RUV_CVCP
 ADD=RUV_SDCP
 SDCP=SQRT(PROP*PROP + ADD*ADD)*EXP(PPV_RUVCP)

   Y=CP + SDCP*EPS1

$TABLE ID TIME WT CL V  Y AGE MDV PNA PMA GEST
ONEHEADER NOPRINT FILE=fentanyl.fit
```

Appendix 3: NM-TRAN code for a 2-compartment population pharmacokinetic used for simulation of Study 3

```
---------------------------------------------------------------------------------------------------------------------

$PROB SIM Fentanyl children 1day Johnson cmt

$DATA fentanyl_Johnson_child_1day_1cmt.csv IGNORE #

$INPUT ID TIME AMT DUR RATE CMT OCC MDV DVID DV AGE WT HT SEX FORM PNA PMA
GEST

$SIM (1234567 NEW) ONLYSIM SUB=1

; Johnson KL, Erickson JP, Holley FO, Scott JC. FENTANYL PHARMACOKINETICS
IN THE PEDIATRIC POPULATION. Anesthesiology. 1984;61(3):A441-A.


$THETA (0.01,0.051,100)      ; CL

$THETA (1,18.9,200)        ; V


;Residual unidentified variability

$THETA 0 FIX ; RUV_SDCP

$THETA 0 FIX ; RUV_CVCP


$OMEGA 0.3  ; PPVCL

$OMEGA 0.2  ; PPVV


;Residual Unidentified Variability (Observations)

$OMEGA 0 FIX ; PPV_RUVCP


; residual error

$SIGMA 1. FIX ; EPS1


$SUBR ADVAN1 TRANS2

$PK

IF (NEWIND.LE.1) THEN    ; sets dose to 0 when start new patient

   LN2=LOG(2)
```

```
   DOSE=0                ; gives doses in output
 ENDIF



   FSZV= 1;WT/70
   FSZCL= 1; FSZV**0.75
   FSZT= 1;FSZV**0.25


    CL=FSZCL*CL*EXP(PPVCL)


   V=FSZV*V*EXP(PPVV)


 $ERROR


  CP=A(1)/V


 PROP=CP*RUV_CVCP
 ADD=RUV_SDCP
 SDCP=SQRT(PROP*PROP + ADD*ADD)*EXP(PPV_RUVCP)


   Y=CP + SDCP*EPS1



$TABLE ID TIME WT CL V  Y AGE MDV PNA PMA GEST
ONEHEADER NOPRINT FILE=fentanyl.fit
```

Appendix 4: NM-TRAN code for a 2-compartment population pharmacokinetic used for simulation of Study 4

```
-----------------------------------------------------------------------------------------------------------------------

$PROB SIM Fentanyl adult 2 cmt

$DATA fentanyl_Foster_adult_2cmt.csv IGNORE #

$INPUT ID TIME AMT DURATION RATE CMT OCC MDV DVID DV AGE WT HT SEX FORM PNA
PMA GEST

$SIM (1234567 NEW) ONLYSIM SUB=1

; Foster D, Upton R, Christrup L, Popper L. Pharmacokinetics and
pharmacodynamics of intranasal versus intravenous fentanyl in patients with
pain after oral surgery. Annals of Pharmacotherapy. 2008;42(10):1380-7.


$THETA (0.1,0.661, 100)      ; CL

$THETA (1,9.07, 200)        ; V1

$THETA (0.1,0.918,300)       ; Q

$THETA (2,63,300)         ; V2


;Residual unidentified variability

$THETA 0 FIX ; RUV_SDCP

$THETA 0 FIX ; RUV_CVCP


$OMEGA 0.3  ; PPVCL

$OMEGA 0.2 ; PPVV1

$OMEGA 0.2  ; PPVV2

$OMEGA 0 FIX ; PPVQ

;Residual Unidentified Variability (Observations)

$OMEGA 0 FIX ; PPV_RUVCP
```

```
; residual error
$SIGMA 1. FIX ; EPS1


$SUBR ADVAN3 TRANS4
$PK
IF (NEWIND.LE.1) THEN    ; sets dose to 0 when start new patient
   LN2=LOG(2)
   DOSE=0                ; gives doses in output
 ENDIF


   FSZV=WT/70
   FSZCL=FSZV**0.75
   FSZT=FSZV**0.25


   CL=FSZCL*CL*EXP(PPVCL)
   Q=FSZCL*Q*EXP(PPVQ)
   V1=FSZV*V1*EXP(PPVV1)
   V2=FSZV*V2*EXP(PPVV2)


  S1=V1


 $ERROR


  CP=A(1)/S1
```

```
 PROP=CP*RUV_CVCP

 ADD=RUV_SDCP

 SDCP=SQRT(PROP*PROP + ADD*ADD)*EXP(PPV_RUVCP)


   Y=CP + SDCP*EPS1


$TABLE ID TIME WT CL V1 Q V2 Y AGE MDV DVID PNA PMA GEST

ONEHEADER NOPRINT FILE=fentanyl.fit
```

Appendix 5: NM-TRAN code for a 3-compartment pharmacokinetic model used for the simulation of Study 5

```
$PROB SIM Fentanyl adult 3 cmt
$DATA fentanyl_Loughren_adult_3cmt.csv IGNORE #
$INPUT ID TIME AMT DUR RATE CMT OCC MDV DVID DV AGE WT HT SEX FORM PNA PMA
GEST
$SIM (1234567 NEW) ONLYSIM SUB=1
; Loughren MJ, Kharasch ED, Kelton-Rehkopf MC, Syrjala KL, Shen DD.
Influence of St. John’s wort on intravenous fentanyl pharmacokinetics,
pharmacodynamics, and clinical effects: a randomized clinical trial.
Anesthesiology. 2020;132(3):491-503.


$THETA (0.1,0.522, 100)      ; CL
$THETA (1,32, 200)        ; V1
$THETA (0.1,0.957, 150)       ; Q2
$THETA (2,19.8, 200)         ; V2
$THETA (0.1,0.799, 150)     ; Q3
$THETA (2,147., 1000) ; V3

;Residual unidentified variability
$THETA (0,0.0174,) ; RUV_SDCP
$THETA (0,0.219,) ; RUV_CVCP


$OMEGA 0.0445 ; PPVCL
$OMEGA 0.0867 ; PPVV1
$OMEGA 0.0884 ; PPVQ2
$OMEGA 0.286 ; PPVV2
$OMEGA 0.189 ; PPVQ3
$OMEGA 0.134 ; PPVV3


;Residual Unidentified Variability (Observations)
$OMEGA 0 FIX ; PPV_RUVCP

; residual error
$SIGMA 1. FIX ; EPS1
```

```
$SUBR ADVAN11 TRANS4
$PK
IF (NEWIND.LE.1) THEN    ; sets dose to 0 when start new patient
   LN2=LOG(2)
   DOSE=0                ; gives doses in output
 ENDIF


   FSZV=WT/70
   FSZCL=FSZV**0.75
   FSZT=FSZV**0.25

   CL=FSZCL*CL*EXP(PPVCL)
   Q2=FSZCL*Q2*EXP(PPVQ2)
   V1=FSZV*V1*EXP(PPVV1)
   V2=FSZV*V2*EXP(PPVV2)
   Q3=FSZCL*Q3*EXP(PPVQ3)
   V3=FSZV*V3*EXP(PPVV3)
  S1=V1

 $ERROR

  CP=A(1)/S1

 PROP=CP*RUV_CVCP
 ADD=RUV_SDCP
 SDCP=SQRT(PROP*PROP + ADD*ADD)*EXP(PPV_RUVCP)

   Y=CP + SDCP*EPS1


$TABLE ID TIME WT CL V1 Q2 V2 V3 Q3 Y AGE MDV PNA PMA GEST
ONEHEADER NOPRINT FILE=fentanyl.fit
```

Appendix 6: NM-TRAN code for a 2-compartment pharmacokinetic model used for the simulation of Study 6

```
-----------------------------------------------------------------------------------------------------------------

$PROB SIM Fentanyl adult 2 cmt

$DATA fentanyl_Scott_adult_2cmt.csv IGNORE #

$INPUT ID TIME AMT DUR RATE CMT OCC MDV DVID DV AGE WT HT SEX FORM PNA PMA
GEST

$SIM (1234567 NEW) ONLYSIM SUB=1

; Scott JC, Stanski D. Decreased fentanyl and alfentanil dose requirements
with age. A simultaneous pharmacokinetic and pharmacodynamic evaluation. J
Pharmacol Exp Ther. 1987;240(1):159-66.


$THETA (0.01, 0.207, 5)      ; CL

$THETA (1, 14.65, 100)        ; V1

$THETA (0.01, 0.268, 5)       ; Q

$THETA (2, 386, 1000)         ; V2


;Residual unidentified variability

$THETA (0,0.01,) ; RUV_SDCP

$THETA (0,0.05,) ; RUV_CVCP


$OMEGA 0.2   ; PPVCL

$OMEGA 0.2    ; PPVV1

$OMEGA 0.2   ; PPVV2

$OMEGA 0 FIX  ; PPVQ

;Residual Unidentified Variability (Observations)

$OMEGA 0 FIX ; PPV_RUVCP


; residual error

$SIGMA 1. FIX ; EPS1


$SUBR ADVAN3 TRANS4
```

```
$PK
IF (NEWIND.LE.1) THEN    ; sets dose to 0 when start new patient
   LN2=LOG(2)
   DOSE=0                ; gives doses in output
 ENDIF

   FSZV=WT/70
   FSZCL=FSZV**0.75
   FSZT=FSZV**0.25

   CL=FSZCL*CL*EXP(PPVCL)
   Q=FSZCL*Q*EXP(PPVQ)
   V1=FSZV*V1*EXP(PPVV1)
   V2=FSZV*V2*EXP(PPVV2)

  S1=V1

 $ERROR
  CP=A(1)/S1

 PROP=CP*RUV_CVCP
 ADD=RUV_SDCP
 SDCP=SQRT(PROP*PROP + ADD*ADD)*EXP(PPV_RUVCP)

   Y=CP + SDCP*EPS1

$TABLE ID TIME WT CL V1 Q V2 Y AGE MDV PNA PMA GEST
ONEHEADER NOPRINT FILE=fentanyl.fit
```

Appendix 7: NM-TRAN code for a 2-compartment pharmacokinetic model used for the simulation of Study 7

```
-----------------------------------------------------------------------------------------------------------------------

$PROB SIM Fentanyl adult 2 cmt

$DATA fentanyl_Lim_adult_IN_IV_2cmt.csv IGNORE #

$INPUT ID OID=DROP TIME AMT RATE DUR OCC MDV DVID DV CMT AGE WT HT SEX PNA
PMA GEST ASY FORM

$SIM (1234567 NEW) ONLYSIM SUB=1

; Lim S, Paech MJ, Sunderland VB, Roberts MJ, Banks SL, Rucklidge MW.
Pharmacokinetics of nasal fentanyl. Journal of Pharmacy Practice and
research. 2003;33(1):59-64.


$THETA (0.1,2.4, 25)    ; CL

$THETA (5,27,200)       ; V1

$THETA (0.1,5.1,200)     ; Q

$THETA (5,32.6,500)     ; V2


;RESIDUAL UNIDETIFIED VARIABILITY ON PLASMA CONCENTRATIONS

$THETA (0.01,0.06,)   ;RUV_CVCP

$THETA (0.0001,0.02,) ;RUV_SDCP


$OMEGA 0.3 ; PPVCL

$OMEGA 0.25 ; PPVV1

$OMEGA 0.3 ; PPVV2

$OMEGA 0.25 ;PPVQ


$OMEGA 0 FIX ;PPV_RUVCP

;Residual error
```

```
$SIGMA 1. FIX ; EPS1



$SUBR ADVAN3 TRANS4


$PK
IF (NEWIND.LE.1) THEN    ; sets dose to 0 when start new patient
   LN2=LOG(2)
   DOSE=0                ; gives doses in output
 ENDIF


   FSZV=WT/70
   FSZCL=FSZV**0.75
   FSZT=FSZV**0.25


   CL=FSZCL*CL*EXP(PPVCL)
   Q=FSZCL*Q*EXP(PPVQ)
   V2=FSZV*V2*EXP(PPVV2)
   V3=FSZV*V3*EXP(PPVV3)


$ERROR
  CP=A(2)/S2
    PROP=CP*RUV_CVCP
    ADD=RUV_SDCP
    SDCP=SQRT(PROP*PROP + ADD*ADD)*EXP(PPV_RUVCP)
```

```
    Y=CP + SDCP*EPS1



$TABLE ID TIME WT CL V2 Q V3 Y AGE MDV DVID PNA PMA GEST KA

ONEHEADER NOPRINT FILE=fentanyl.fit
```

Appendix 8: NM-TRAN code for final 1-compartment model used in PK analysis of IV fentanyl

```
-----------------------------------------------------------------------------------------------------------------

$PROBLEM 1CMT IV FENTANYL (WFN EXTENDED FORMAT)

$INPUT ID OID TIME AMT DUR RATE MDV DVID DV AGE WT HT SEX PNA PMA GA ASY

$DATA ..\Fentanyl_PK_combined_1cmt.csv IGNORE=#

$ESTIM  MAXEVAL=9999    NSIG=3  SIGL=9  PRINT=1  NOABORT  METHOD=CONDITIONAL
INTERACTION

$COV


$SUB ADVAN1 TRANS2


$THETA (0.01,1.41, 5)       ; POP_CL

$THETA (10,60.2, 250)       ; POP_V


$THETA (20,47.1,100)      ; T50CL

$THETA (0.5,3.52,10)       ; HILLCL


$THETA (0.1,7.49,100)      ; CONVD

$THETA (0.05,258.,)       ; TVOL


;RESIDUAL UNIDENTIFIED VARIABILITY

$THETA (0,0.00863,)  ; RUV_SDCP

$THETA (0,0.389,) ; RUV_CVCP
```

```
$OMEGA BLOCK (2)
0.562 ; PPVCL
0.232 0.596 ; PPVV

$OMEGA 0 FIX            ; PPV_RUVCP

$SIGMA 1. FIX ; EPS1

$PK
LN2=LOG(2)
FSZCL=(WT/70)**.75
FSZV=WT/70

 TDEVCL=THETA(3)
  HCL=THETA(4)
  TDHCL=TDEVCL**HCL
  PMAHIL=PMA**HCL
CLAGE=PMAHIL/(PMAHIL+TDHCL) ; PMA WEEKS

CL=FSZCL* CLAGE* THETA(1) * EXP(ETA(1))

IF (PNA.LE.0) THEN
     VAGE=1
   ELSE
     VAGE=1+THETA(5)*EXP(-PNA*0.693/THETA(6))  ; PNA WEEKS
 ENDIF
```

```
V=FSZV * VAGE * THETA(2) * EXP(ETA(2))


S1=V

$ERROR

       CP=A(1)/S1


   PROP=CP*THETA(8)

   ADD=THETA(7)

   SDCP=SQRT(PROP*PROP + ADD*ADD)*EXP(ETA(3))

   Y=CP + SDCP*ERR(1)


$TABLE ID TIME WT CL V DVID Y PMA GA PNA

ONEHEADER NOPRINT FILE=fentanyl_pk_combined_1cmt_pmacl_pnav.fit
```

Appendix 9: NM-TRAN code for final 2-compartment model used in PK analysis of IV fentanyl

```
-----------------------------------------------------------------------------------------------------

$PROBLEM 2CMT IV FENTANYL (WFN EXTENDED FORMAT)

$INPUT ID OID=DROP TIME AMT DUR RATE MDV CMT DVID DV AGE WT HT SEX PNA PMA
GA ASY

$DATA ..\Fentanyl_PK_combined_2cmt.csv IGNORE=#

$ESTIM MAXEVAL=9999   NSIG=5  SIGL=9  PRINT=1  NOABORT  METHOD=CONDITIONAL
INTERACTION

$COV


$SUB ADVAN3 TRANS4


$THETA (0.01,1.42, 5)      ; POP_CL

$THETA (1,36.5, 250)      ; POP_V1

$THETA (0.01,3.23, 150)       ; POP_Q

$THETA (10,96.3, 300)           ; POP_V2


$THETA (30,45.2,60)     ; T50CL

$THETA (0.5,4.1,10)      ; HILLCL


$THETA (0.1,8.28,100)     ; CONVD1

$THETA (0.05,227.,)      ; TVOL1


$THETA (0.1,0.765,100)     ; CONVD2

$THETA (0.05,2.24,)      ; TVOL2
```

```
;RESIDUAL UNIDENTIFIED VARIABILITY
$THETA (0,0.0367,)  ; RUV_SDCP
$THETA (0,0.106,) ; RUV_CVCP

$OMEGA BLOCK (4)
0.471 ; PPVCL
0.184 1.02 ; PPVV1
0.00631 0.712 2.08 ; PPVVQ
0.403 -0.233 -1.19 1.3 ; PPVV2

$OMEGA 0 FIX             ; PPV_RUVCP

$SIGMA 1. FIX ; EPS1

$PK
FSZCL=(WT/70)**.75
FSZV=WT/70
LN2=LOG(2)

 TDEVCL=THETA(5)
  HCL=THETA(6)
  TDHCL=TDEVCL**HCL
  PMAHIL=PMA**HCL
CLAGE=PMAHIL/(PMAHIL+TDHCL) ; PMA WEEKS
CL=FSZCL* CLAGE * THETA(1) * EXP(ETA(1))
```

```
IF (PNA.LE.0) THEN
     VAGE1=1
     VAGE2=1
   ELSE
     VAGE1=1+THETA(7)*EXP(-PNA*LN2/THETA(8))  ; PNA WEEKS
     VAGE2=1+THETA(9)*EXP(-PNA*LN2/THETA(10))
 ENDIF

V1=FSZV * VAGE1 * THETA(2) * EXP(ETA(2))
Q=FSZCL* THETA(3) * EXP(ETA(3))
V2=FSZV * VAGE2* THETA(4) * EXP(ETA(4))
S1=V1
S2=V2

$ERROR
       CP=A(1)/S1

   PROP=CP*THETA(12)
   ADD=THETA(11)
   SDCP=SQRT(PROP*PROP + ADD*ADD)*EXP(ETA(5))
   Y=CP + SDCP*ERR(1)

$TABLE ID TIME WT CL V1 Q V2 DVID Y PMA GA PNA
ONEHEADER NOPRINT FILE=fentanyl_pk_combined_2cmt_pmacl_pnav1v2.fit
```

Appendix 10: NM-TRAN code for final 3-compartment model used in PK analysis of IV fentanyl

---

```
$PROBLEM 3CMT IV FENTANYL (WFN EXTENDED FORMAT)

$INPUT ID OID=DROP TIME AMT DUR RATE MDV CMT DVID DV AGE WT HT SEX PNA PMA
GA ASY

$DATA ..\Fentanyl_PK_combined_3cmt.csv IGNORE=#

$ESTIM  MAXEVAL=9999    NSIG=5  SIGL=9  PRINT=1  NOABORT  METHOD=CONDITIONAL
INTERACTION

$COV


$SUB ADVAN11 TRANS4


$THETA (0.01,1.29, 5)      ; POP_CL

$THETA (1,35., 250)      ; POP_V1

$THETA (0.01,3.4, 150)       ; POP_Q2

$THETA (10,82.1, 300)           ; POP_V2

$THETA (0.001,0.0516,1)       ; POP_Q3

$THETA (0.1,509., 1000)           ; POP_V3


$THETA (0.1,8.27,100)     ; CONVD1

$THETA (0.05,205.,)      ; TVOL1


$THETA (0.1,0.692,100)     ; CONVD2

$THETA (0.05,13.9,)      ; TVOL2
```

```
$THETA (0.005,0.493,50)     ; CONVD3
$THETA (0.1 ,58.,)      ; TVOL3

$THETA (30,51.4,60)     ; T50CL
$THETA (0.5,3.59,10)      ; HILLCL

;RESIDUAL UNIDENTIFIED VARIABILITY
$THETA (0.0386)  ; RUV_SDCP
$THETA (0.104) ; RUV_CVCP

$OMEGA BLOCK (6)
0.727 ; PPVCL
0.278 1.07 ; PPVV1
0.117 0.766 2.03 ; PPVQ2
0.572 -0.248 -1.38 1.77 ; PPVV2
0.689 -0.154 0.307 -1.41 2.65 ; PPVV3
0.541 -0.365 -0.211 -0.411 0.615 0.654 ; PPVQ3



$OMEGA 0 FIX                                          ; PPV_RUVCP

$SIGMA 1. FIX ; EPS1

$PK
FSZCL=(WT/70)**.75
```

```
FSZV=WT/70

LN2=LOG(2)


 TDEVCL=THETA(13)

  HCL=THETA(14)

  TDHCL=TDEVCL**HCL

  PMAHIL=PMA**HCL

CLAGE=PMAHIL/(PMAHIL+TDHCL) ; PMA WEEKS


CL=FSZCL* CLAGE* THETA(1) * EXP(ETA(1))


IF (PNA.LE.0) THEN

     VAGE1=1

     VAGE2=1

     VAGE3=1

   ELSE

     VAGE1=1+THETA(7)*EXP(-PNA*LN2/THETA(8))  ; PNA WEEKS

     VAGE2=1+THETA(9)*EXP(-PNA*LN2/THETA(10))

     VAGE3=1+THETA(11)*EXP(-PNA*LN2/THETA(12))

 ENDIF


V1=FSZV * VAGE1 * THETA(2) * EXP(ETA(2))

Q2=FSZCL* THETA(3) * EXP(ETA(3))

V2=FSZV * VAGE2 * THETA(4) * EXP(ETA(4))

Q3=FSZCL* THETA(5) * EXP(ETA(6))

V3=FSZV * VAGE3 * THETA(6) * EXP(ETA(5))
```

```
S1=V1

S2=V2

S3=V3


$ERROR

       CP=A(1)/S1


   PROP=CP*THETA(16)

   ADD=THETA(15)

   SDCP=SQRT(PROP*PROP + ADD*ADD)*EXP(ETA(7))

   Y=CP + SDCP*ERR(1)


$TABLE ID TIME WT CL V1 Q2 V2 Q3 V3 DVID Y PMA GA PNA

ONEHEADER NOPRINT FILE=fentanyl_pk_combined_3cmt_pmacl_pnav1v2v3.fit
```

Appendix 11: NM-TRAN code for final 3-compartment model used in PK analysis of nasal + oral fentanyl

---

```
$PROB 2CMT ORAL FENTANYL (WFN EXTENDED FORMAT)

$DATA ..\Fentanyl_PK_combined_IV_IN_Oral_3cmt.csv IGNORE #

$INPUT ID OID=DROP TIME AMT DUR RATE MDV CMT DVID DV AGE WT HT SEX PNA PMA
GA ASY FORM OCC

$ESTIM MAXEVAL=9999 NSIG=5 SIGL=9 PRINT=0 NOABORT METHOD=CONDITIONAL
INTERACTION

$COV


$THETA (0.01,1.29, 5)   FIX   ; CL

$THETA (1,35., 250)   FIX   ; V2

$THETA (0.01,3.4, 150)   FIX    ; Q3

$THETA (10,82.1, 300)    FIX       ; V3

$THETA (0.001,0.0516,1)   FIX    ; Q4

$THETA (0.1,509., 1000)    FIX       ; V4


$THETA 0.004 FIX ; POPTK0 H

$THETA (0.001,7.45,30)   ; TABPO

$THETA (0.01,5.99,10)     ; LAG

$THETA (0.1,0.42, 1) ; FPO

$THETA (0.01,7.69,30)   ; TABN

$THETA (0.01,2.58, 10)     ; LAGN

$THETA (0.01,0.904, 1)   ; FPN
```

```
$THETA (0.1,8.27,100)  FIX   ; CONVD2
$THETA (0.05,205.,)    FIX   ; TVOL2

$THETA (0.1,0.692,100)  FIX   ; CONVD3
$THETA (0.05,13.9,)    FIX   ; TVOL3



$THETA (0.005,0.493,50)  FIX   ; CONVD4
$THETA (0.1 ,58.,)    FIX   ; TVOL4

$THETA (30,51.4,60)  FIX   ; T50CL
$THETA (0.5,3.59,10)   FIX   ; HILLCL



;RESIDUAL UNIDENTIFIED VARIABILITY
$THETA (0,0.0273,) ; RUV_SDCP
$THETA (0,0.124,) ; RUV_CVCP



$OMEGA BLOCK (5)
0.66 ; PPVCL
0.501 1.95 ; PPVV2
0.408 0.634 0.627 ; PPVQ3
0.137 -0.451 -0.0847 1.6 ; PPVV3
-0.00112 -0.181 -0.0997 0.0709 0.458 ; PPVV4
```

```
$OMEGA 0.2                    ; PPVQ4

$OMEGA 0.2                    ; PPVTABN

$OMEGA 0 FIX                     ; PPVTK0

$OMEGA 0.219                   ; PPVLAG

$OMEGA 0 FIX                     ; PPVFPO

$OMEGA 0.2                    ; PPVTABPO

$OMEGA 0.2                    ; PPVLGN

$OMEGA 0 FIX                     ; PPVFPN


$OMEGA 0 FIX                     ; PPV_RUVCP


$SIGMA 1. FIX ; EPS1


$SUBR ADVAN12 TRANS4
;$MODEL
  ; COMP(DEPOT)      ; DEPOT for enteral
  ; COMP(PLASMA)     ; central
  ; COMP(PERI)    ; peripheral


$PK


IF (NEWIND.LE.1) THEN    ; SETS DOSE TO 0 WHEN START NEW PATIENT
   LN2=LOG(2)
   DOSE=0                ; GIVES DOSES IN OUTPUT
 ENDIF
```

```
A_0(1)=0

A_0(2)=0

A_0(3)=0


   FSZV=WT/70

   FSZCL=FSZV**0.75

   FSZT=FSZV**0.25

   LN2=LOG(2)


  TDEVCL=THETA(14)

  HCL=THETA(15)

  TDHCL=TDEVCL**HCL

  PMAHIL=PMA**HCL

CLAGE=PMAHIL/(PMAHIL+TDHCL)




   CL=FSZCL*CLAGE*THETA(1)*EXP(ETA(1))

   Q3=FSZCL*THETA(4)*EXP(ETA(3))

   Q4=FSZCL*THETA(6)*EXP(ETA(6))


  IF (PNA.LE.0) THEN

     VAGE2=1

     VAGE3=1

     VAGE4=1

   ELSE

     VAGE2=1+THETA(16)*EXP(-PNA*LN2/THETA(17))
```

```
    VAGE3=1+THETA(18)*EXP(-PNA*LN2/THETA(19))
    VAGE4=1+THETA(20)*EXP(-PNA*LN2/THETA(21))
ENDIF

  V2=FSZV * VAGE2 * THETA(2) * EXP(ETA(2))
  V3=FSZV * VAGE3 * THETA(3) * EXP(ETA(4))
  V4=FSZV * VAGE4 * THETA(5) * EXP(ETA(5))

  TK0=THETA(7)*EXP(ETA(8))

 IF (FORM.EQ.2) THEN
   TABS=THETA(11)*EXP(ETA(7))
   F1=THETA(13)*EXP(ETA(13))
   ALAG1=THETA(12)*EXP(ETA(12))
  ENDIF

  IF (FORM.EQ.3) THEN
    TABS=THETA(8)*EXP(ETA(11))
    F1=THETA(10)*EXP(ETA(10))
    ALAG1=THETA(9)*EXP(ETA(9))
  ENDIF

     KA=LN2/TABS
  S2=V2
  D2=TK0
```

```
$ERROR


  CP=A(2)/S2


   PROP=CP*THETA(23)

   ADD=THETA(22)

   SDCP=SQRT(PROP*PROP + ADD*ADD)*EXP(ETA(14))

   Y=CP + SDCP*ERR(1)


$TABLE ID TIME WT CL V2 V3 Q3 V4 Q4 TABS ALAG1 F1 Y AGE PNA MDV

ONEHEADER                                                              NOPRINT
FILE=fentanyl_pk_combined_3cmt_iv_in_oral_pmacl_pnav1v2v3-5block.fit
```

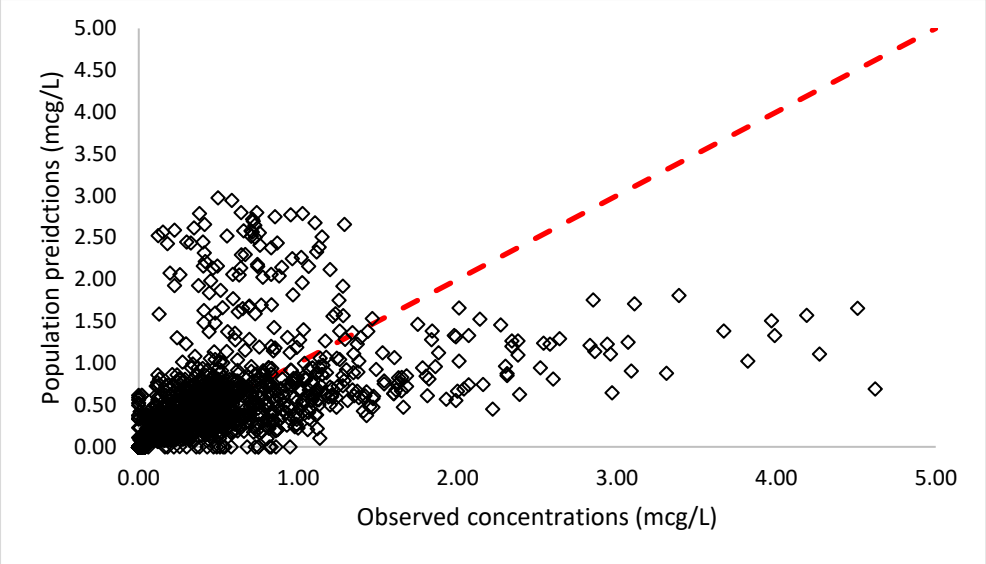

Appendix 12: Comparison of population predicted and observed fentanyl concentrations for IV nasal and oral data. Dotted shapes represent each individual. Dashed red line represents the line of identity.

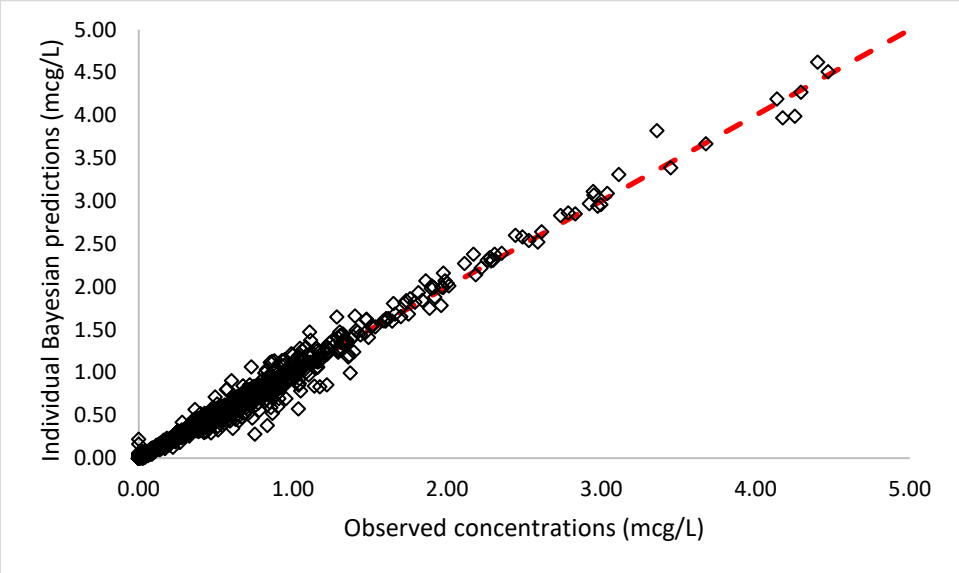

Appendix 13: Comparison of individual Bayesian predicted and observed fentanyl concentrations for IV,nasal and oral data only. Dotted shapes represent each individual. Dashed red line indicates the line of identity

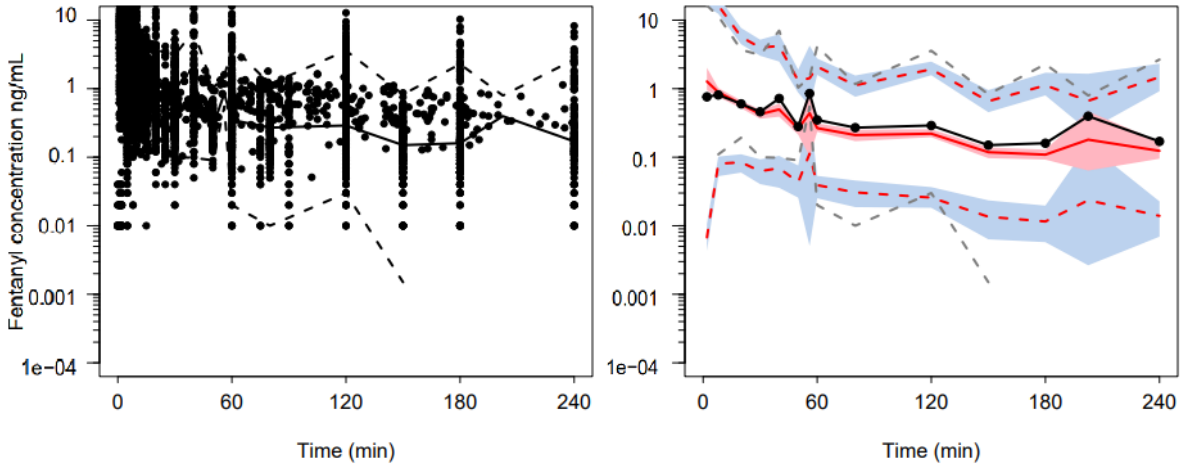

Appendix 14: Visual predictive check for the final three-compartment pharmacokinetic model. All plots shows median (solid lines) and 90% intervals (dashed lines). The plot of the left shows the observed fentanyl concentrations. The plot on the right shows the 10^{th}, 50^{th} and 90^{th} percentiles for the predictions (red-dashed lines) overlaid with the 10^{th}, 50^{th} and 90^{th} percentiles for the observations (grey-dashed line). The blue shaded areas represent the 95% confidence intervals for the prediction percentiles.

References

1. Sposito NPB, Rossato LM, Bueno M, Kimura AF, Costa T, Guedes DMB. Assessment and management of pain in newborns hospitalized in a Neonatal Intensive Care Unit: a cross-sectional study. Revista latino-americana de enfermagem. 2017;25.
2. Weesie YM, van Dijk L, Bouvy ML, Hek K. Immediate release fentanyl in general practices: Mostly off-label prescribing. European Journal of General Practice. 2023;29(1):2165644.
3. Williams MD, Lascelles BDX. Early neonatal pain—a review of clinical and experimental implications on painful conditions later in life. Frontiers in Pediatrics. 2020;8:30.
4. Berde CB, Sethna NF. Analgesics for the treatment of pain in children. New England Journal of Medicine. 2002;347(14):1094-103.
5. Rosen DM, Alcock MM, Palmer GM. Opioids for acute pain management in children. Anaesthesia and Intensive Care. 2022;50(1-2):81-94.
6. Saarenmaa E, Huttunen P, Leppäluoto J, Meretoja O, Fellman V. Advantages of fentanyl over morphine in analgesia for ventilated newborn infants after birth: a randomized trial. The Journal of pediatrics. 1999;134(2):144-50.
7. Holford N, Heo Y-A, Anderson B. A Pharmacokinetic Standard for Babies and Adults. Journal of Pharmaceutical Sciences. 2013;102(9):2941-52 %U https://www.sciencedirect.com/science/article/pii/S0022354915309357.
8. Lee B, Park JD, Choi YH, Han YJ, Suh DI. Efficacy and safety of fentanyl in combination with midazolam in children on mechanical ventilation. Journal of Korean Medical Science. 2019;34(3).
9. NZ M. Fentanyl MEDSAFE Datasheet 2024. Available from: https://www.medsafe.govt.nz/profs/datasheet/f/FentanylSolforinj.pdf
10. Kennedy RM, Luhmann JD. Pharmacological management of pain and anxiety during emergency procedures in children. Paediatric drugs. 2001;3:337-54.
11. Nave R, Schmitt H, Popper L. Faster absorption and higher systemic bioavailability of intranasal fentanyl spray compared to oral transmucosal fentanyl citrate in healthy subjects. Drug delivery. 2013;20(5):216-23 %U https://doi.org/10.3109/10717544.2012.762435.
12. Watts P, Smith A, Perelman M. Nasal delivery of fentanyl. Drug delivery and translational research. 2013;3(1):75-83.
13. Holford NH. Target concentration intervention: beyond Y2K. British Journal of Clinical Pharmacology. 2001;52(S1):55-9.
14. Meibohm B, Derendorf H. Basic concepts of pharmacokinetic/pharmacodynamic (PK/PD) modelling. International journal of clinical pharmacology and therapeutics. 1997;35(10):401-13.
15. Zierler K. A critique of compartmental analysis. Annual Review of Biophysics and Bioengineering. 1981;10(1):531-62.
16. DiStefano 3rd J. Noncompartmental vs. compartmental analysis: some bases for choice. American Journal of Physiology-Regulatory, Integrative and Comparative Physiology. 1982;243(1):R1-R6.
17. FOSTER DM. Noncompartmental versus compartmental approaches to pharmacokinetic analysis. In: Principles of clinical pharmacology. Elsevier; 2007. p. 89-105.
18. Wolfsegger MJ, Jaki T. Non-compartmental estimation of pharmacokinetic parameters in serial sampling designs. Journal of pharmacokinetics and pharmacodynamics. 2009;36:479-94.
19. Wang Z, Kim S, Quinney SK, Zhou J, Li L. Non-compartment model to compartment model pharmacokinetics transformation meta-analysis–a multivariate nonlinear mixed model. BMC Systems Biology. 2010;4(1):1-7.
20. Ariano RE, Duke PC, Sitar DS. Population pharmacokinetics of fentanyl in healthy volunteers. The Journal of Clinical Pharmacology. 2001;41(7):757-63.
21. Mather L, Gourlay G. Pharmacokinetics of fentanyl. In: Transdermal fentanyl: a new approach to prolonged pain control. Springer; 1991. p. 73-97.

22. Singleton M, Rosen J, Fisher D. Pharmacokinetics of fentanyl in the elderly. British journal of anaesthesia. 1988;60(6):619-22.
23. Foster DM, Vicini P. Noncompartmental and compartmental approaches to pharmacokinetic data analysis. In: Atkinson's Principles of Clinical Pharmacology. Elsevier; 2022. p. 113-35.
24. Jaki T, Wolfsegger MJ. Non‐compartmental estimation of pharmacokinetic parameters for flexible sampling designs. Statistics in Medicine. 2012;31(11-12):1059-73.
25. Anderson BJ, Potts A, Herd DW. Problems and pitfalls performing PK studies in children. PPDT. 2007;8:4-17.
26. Ette EI, Williams PJ. Population pharmacokinetics I: background, concepts, and models. Annals of Pharmacotherapy. 2004;38(10):1702-6.
27. Anderson BJ, Allegaert K, Holford NH. Population clinical pharmacology of children: general principles. Eur J Pediatr. 2006;165(11):741-6.
28. Carter AA, Rosenbaum SE, Dudley MN. Review of methods in population pharmacokinetics. Clinical research and regulatory affairs. 1995;12(1):1-21.
29. Anderson BJ, Allegaert K, Holford NH. Population clinical pharmacology of children: modelling covariate effects. Eur J Pediatr. 2006;165(12):819-29.
30. Cortínez LI, Anderson BJ. Modeling the pharmacokinetics and pharmacodynamics of sevoflurane using compartment models in children and adults. Pediatric Anesthesia. 2018;28(10):834-40 %U https://onlinelibrary.wiley.com/doi/abs/10.1111/pan.13465.
31. Duffull S, Waterhouse T, Eccleston J. Some considerations on the design of population pharmacokinetic studies. J Pharmacokinet Pharmacodyn. 2005;32(3-4):441-57.
32. Peck CC, Sheiner LB, Nichols AI. The problem of choosing weights in nonlinear regression analysis of pharmacokinetic data. Drug Metabolism Reviews. 1984;15(1 & 2):133-48.
33. Peck CC, Beal SL, Sheiner LB, Nichols AI. Extended least squares nonlinear regression: A possible solution to the "choice of weights" problem in analysis of individual pharmacokinetic parameters. Journal of Pharmacokinetics and Biopharmaceutics. 1984;12(5):545-57.
34. Anderson BJ, Lerman J, Coté CJ. 7 - Pharmacokinetics and Pharmacology of Drugs Used in Children. In: Coté CJ, Lerman J, Anderson BJ, editors. A Practice of Anesthesia for Infants and Children (Sixth Edition). Philadelphia: Elsevier; 2019. p. 100-76.e45 %@ 978-0-323-42974-0 %U https://www.sciencedirect.com/science/article/pii/B9780323429740000070.
35. Ziesenitz VC, Vaughns JD, Koch G, Mikus G, van den Anker JN. Pharmacokinetics of Fentanyl and Its Derivatives in Children: A Comprehensive Review. Clinical pharmacokinetics. 2018;57(2):125-49.
36. De Cock RFW, Piana C, Krekels EHJ, Danhof M, Allegaert K, Knibbe CAJ. The role of population PK–PD modelling in paediatric clinical research. European Journal of Clinical Pharmacology. 2011;67(Suppl 1):5-16 %U https://www.ncbi.nlm.nih.gov/pmc/articles/PMC3082690/.
37. Anderson BJ, Holford NH. Mechanism-based concepts of size and maturity in pharmacokinetics. Annu Rev Pharmacol Toxicol. 2008;48:303-32.
38. Anderson BJ, Holford NH. Mechanistic basis of using body size and maturation to predict clearance in humans. Drug metabolism and pharmacokinetics. 2009;24(1):25-36.
39. Schwartz GJ, Work DF. Measurement and estimation of GFR in children and adolescents. Clinical Journal of the American Society of Nephrology. 2009;4(11):1832-43.
40. O'Hara K, Wright IMR, Schneider JJ, Jones AL, Martin JH. Pharmacokinetics in neonatal prescribing: evidence base, paradigms and the future. British Journal of Clinical Pharmacology. 2015;80(6):1281-8 %U https://www.ncbi.nlm.nih.gov/pmc/articles/PMC4693494/.
41. Anderson BJ, Holford NHG. Understanding dosing: children are small adults, neonates are immature children. Archives of Disease in Childhood. 2013;98(9):737-44.
42. Anderson BJ. Neonatal pharmacology. Anaesthesia & Intensive Care Medicine. 2023;24(1):10-7.
43. Wu Y, Völler S, Flint RB, Simons SH, Allegaert K, Fellman V, et al. Pre-and postnatal maturation are important for fentanyl exposure in preterm and term newborns: a pooled population pharmacokinetic study. Clinical pharmacokinetics. 2022:1-12.
44. Saarenmaa E, Neuvonen PJ, Fellman V. Gestational age and birth weight effects on plasma clearance of fentanyl in newborn infants. The Journal of pediatrics. 2000;136(6):767-70.

45. Völler S, Flint RB, Andriessen P, Allegaert K, Zimmermann LJ, Liem KD, et al. Rapidly maturing fentanyl clearance in preterm neonates. Archives of Disease in Childhood-Fetal and Neonatal Edition. 2019;104(6):F598-F603.
46. Koehntop DE, Rodman JH, Brundage DM, Hegland MG, Buckley JJ. Pharmacokinetics of fentanyl in neonates. Anesthesia & Analgesia. 1986;65(3):227-32.
47. Johnson KL, Erickson JP, Holley FO, Scott JC. FENTANYL PHARMACOKINETICS IN THE PEDIATRIC POPULATION. Anesthesiology. 1984;61(3):A441-A.
48. Foster D, Upton R, Christrup L, Popper L. Pharmacokinetics and pharmacodynamics of intranasal versus intravenous fentanyl in patients with pain after oral surgery. Annals of Pharmacotherapy. 2008;42(10):1380-7.
49. Loughren MJ, Kharasch ED, Kelton-Rehkopf MC, Syrjala KL, Shen DD. Influence of St. John's wort on intravenous fentanyl pharmacokinetics, pharmacodynamics, and clinical effects: a randomized clinical trial. Anesthesiology. 2020;132(3):491-503.
50. Scott JC, Stanski D. Decreased fentanyl and alfentanil dose requirements with age. A simultaneous pharmacokinetic and pharmacodynamic evaluation. J Pharmacol Exp Ther. 1987;240(1):159-66.
51. Lim S, Paech MJ, Sunderland VB, Roberts MJ, Banks SL, Rucklidge MW. Pharmacokinetics of nasal fentanyl. Journal of Pharmacy Practice and research. 2003;33(1):59-64.
52. Jaruratanasirikul S, Boonpeng A, Nawakitrangsan M, Samaeng M. NONMEM population pharmacokinetics and Monte Carlo dosing simulations of imipenem in critically ill patients with life‐threatening severe infections during support with or without extracorporeal membrane oxygenation in an intensive care unit. Pharmacotherapy: The Journal of Human Pharmacology and Drug Therapy. 2021;41(7):572-97.
53. Ginsberg G, Hattis D, Sonawane B, Russ A, Banati P, Kozlak M, et al. Evaluation of child/adult pharmacokinetic differences from a database derived from the therapeutic drug literature. Toxicological Sciences. 2002;66(2):185-200.
54. Mangoni AA, Jackson SH. Age‐related changes in pharmacokinetics and pharmacodynamics: basic principles and practical applications. British journal of clinical pharmacology. 2004;57(1):6-14.
55. Verscheijden LF, Koenderink JB, Johnson TN, de Wildt SN, Russel FG. Physiologically-based pharmacokinetic models for children: Starting to reach maturation? Pharmacology & therapeutics. 2020;211:107541.
56. Post TM, Freijer JI, Ploeger BA, Danhof M. Extensions to the visual predictive check to facilitate model performance evaluation. Journal of pharmacokinetics and pharmacodynamics. 2008;35:185-202.
57. Efron B, Tibshirani R. Bootstrap methods for standard errors, confidence intervals, and other measures of statistical accuracy. Statistical science. 1986:54-75.
58. Parke J, Holford NH, Charles BG. A procedure for generating bootstrap samples for the validation of nonlinear mixed-effects population models. Computer methods and programs in biomedicine. 1999;59(1):19-29.
59. Xu XS, Yuan M, Karlsson MO, Dunne A, Nandy P, Vermeulen A. Shrinkage in nonlinear mixed-effects population models: quantification, influencing factors, and impact. The AAPS journal. 2012;14:927-36.
60. Feierman DE, Lasker JM. Metabolism of fentanyl, a synthetic opioid analgesic, by human liver microsomes. Role of CYP3A4. Drug Metabolism and Disposition. 1996;24(9):932-9.
61. Bentley JB, Borel JD, Nenad Jr RE, Gillespie TJ. Age and fentanyl pharmacokinetics. Anesthesia & Analgesia. 1982;61(12):968-71.
62. Calvier EA, Krekels EH, Välitalo PA, Rostami-Hodjegan A, Tibboel D, Danhof M, et al. Allometric scaling of clearance in paediatric patients: when does the magic of 0.75 fade? Clinical pharmacokinetics. 2017;56:273-85.
63. Eleveld DJ, Koomen JV, Absalom AR, Su H, Hannivoort LN, Struys MM. Allometric scaling in pharmacokinetic studies in anesthesiology. Anesthesiology. 2022;136(4):609-17.
64. Anderson BJ, Larsson P. A maturation model for midazolam clearance. Pediatric Anesthesia. 2011;21(3):302-8.

65. Lacroix D, Sonnier M, Moncion A, Cheron G, Cresteil T. Expression of CYP3A in the human liver—evidence that the shift between CYP3A7 and CYP3A4 occurs immediately after birth. European Journal of Biochemistry. 1997;247(2):625-34.
66. Ince I, Knibbe CA, Danhof M, de Wildt SN. Developmental changes in the expression and function of cytochrome P450 3A isoforms: evidence from in vitro and in vivo investigations. Clinical pharmacokinetics. 2013;52:333-45.
67. Joh J, Sila M, Bastani B. Nondialyzability of fentanyl with high-efficiency and high-flux membranes. Anesthesia & Analgesia. 1998;86(2):447.
68. Goldman CA, Snell RR, Thomason JJ, Brown DB. Principles of allometry. Tested studies for laboratory teaching. 1990;11:43-72.
69. Mahmood I. Prediction of clearance, volume of distribution and half-life by allometric scaling and by use of plasma concentrations predicted from pharmacokinetic constants: a comparative study. Journal of pharmacy and pharmacology. 1999;51(8):905-10.
70. Allegaert K, Simons SH, Vanhole C, Tibboel D. Developmental pharmacokinetics of opioids in neonates. Journal of opioid management. 2007;3(1):59-64.
71. Chaplin S, Zeppetella G. Instanyl: intranasal fentanyl for treating breakthrough pain. Prescriber. 2010;21(6):40-2.
72. Levin P. Fentanyl oral and buccal delivery systems. The Essence of Analgesia and Analgesics. 2009;110:131.
73. Schug SA, Ting S. Fentanyl formulations in the management of pain: an update. Drugs. 2017;77:747-63.
74. Mystakidou K, Katsouda E, Parpa E, Tsiatas ML, Vlahos L. Oral transmucosal fentanyl citrate for the treatment of breakthrough pain in cancer patients: an overview of its pharmacological and clinical characteristics. Journal of opioid management. 2005;1(1):36-40.
75. Mystakidou K, Katsouda E, Parpa E, Vlahos L, Tsiatas ML. Oral transmucosal fentanyl citrate: overview of pharmacological and clinical characteristics. Drug delivery. 2006;13(4):269-76.
76. Davis MP. Fentanyl for breakthrough pain: a systematic review. Expert review of neurotherapeutics. 2011;11(8):1197-216.
77. Feld LH, Champeau MW, van Steennis CA, Scott JC. Preanesthetic medication in children: a comparison of oral transmucosal fentanyl citrate versus placebo. Anesthesiology. 1989;71(3):374-7.
78. Lind GH, Marcus MA, Mears SL, Ashburn MA, Peterson BJ, Bernhisel KT, et al. Oral transmucosal fentanyl citrate for analgesia and sedation in the emergency department. Annals of emergency medicine. 1991;20(10):1117-20.
79. Goldstein-Dresner MC, Davis PJ, Kretchman E, Siewers RD, Certo N, Cook DR. Double-blind comparison of oral transmucosal fentanyl citrate with oral meperidine, diazepam, and atropine as preanesthetic medication in children with congenital heart disease. Anesthesiology. 1991;74(1):28-33.
80. Friesen RH, Lockhart CH. Oral transmucosal fentanyl citrate for preanesthetic medication of pediatric day surgery patients with and without droperidol as a prophylactic anti-emetic. Anesthesiology. 1992;76(1):46-51.
81. Epstein RH, Mendel HG, Witkowski TA, Waters R, Guarniari KM, Marr AT, et al. The safety and efficacy of oral transmucosal fentanyl citrate for preoperative sedation in young children. Anesthesia and analgesia. 1996;83(6):1200-5.
82. Malviya S, Voepel-Lewis T, Huntington J, Siewert M, Green W. Effects of anesthetic technique on side effects associated with fentanyl Oralet premedication. Journal of clinical anesthesia. 1997;9(5):374-8.
83. Dsida RM, Wheeler M, Birmingham PK, Henthorn TK, Avram MJ, Enders-Klein C, et al. Premedication of pediatric tonsillectomy patients with oral transmucosal fentanyl citrate. Anesthesia and analgesia. 1998;86(1):66-70.
84. Wheeler M, Birmingham PK, Dsida RM, Wang Z, Coté CJ, Avram MJ. Uptake pharmacokinetics of the Fentanyl Oralet in children scheduled for central venous access removal: implications for the timing of initiating painful procedures. Paediatric anaesthesia. 2002;12(7):594-9.
85. Valtola A, Laakso M, Hakomäki H, Anderson BJ, Kokki H, Ranta V-P, et al. Intranasal fentanyl for intervention-associated breakthrough pain after cardiac surgery. Clinical pharmacokinetics. 2021;60:907-19.

86. Upton RN, Foster DJ, Christrup LL, Dale O, Moksnes K, Popper L. A physiologically-based recirculatory meta-model for nasal fentanyl in man. Journal of pharmacokinetics and pharmacodynamics. 2012;39:561-76.
87. Panagiotou I, Mystakidou K. Intranasal fentanyl: from pharmacokinetics and bioavailability to current treatment applications. Expert review of anticancer therapy. 2010;10(7):1009-21.
88. Streisand JB, Varvel JR, Stanski DR, Le Maire L, Ashburn MA, Hague BI, et al. Absorption and bioavailability of oral transmucosal fentanyl citrate. Anesthesiology. 1991;75(2):223-9.
89. Vasisht N, Gever LN, Tagarro I, Finn AL. Formulation selection and pharmacokinetic comparison of fentanyl buccal soluble film with oral transmucosal fentanyl citrate: a randomized, open-label, single-dose, crossover study. Clinical drug investigation. 2009;29:647-54.
90. Lötsch J, Walter C, Parnham MJ, Oertel BG, Geisslinger G. Pharmacokinetics of non-intravenous formulations of fentanyl. Clinical pharmacokinetics. 2013;52:23-36.
91. Sankar V, Hearnden V, Hull K, Juras DV, Greenberg M, Kerr A, et al. Local drug delivery for oral mucosal diseases: challenges and opportunities. Oral diseases. 2011;17:73-84.